

## Accounts

### Reduction of CO<sub>2</sub> Directed toward Carbon–Carbon Bond Formation

Koji Tanaka

Institute for Molecular Science, Myodaiji, Okazaki 444

(Received June 12, 1997)

This paper describes electrochemical reduction of CO<sub>2</sub> directed toward carbon–carbon bond formation via metal–CO<sub>2</sub> adducts. An electrophilic attack of CO<sub>2</sub> to penta-coordinated low valent polypyridyl Ru complexes affords a Ru– $\eta^1$ -CO<sub>2</sub> adduct, which is easily converted to Ru–CO species either by an acid–base equilibrium in protic media and oxide transfer to CO<sub>2</sub> under aprotic conditions. Two-electron reduction of resultant Ru–CO in protic solutions competitively causes a cleavage of the Ru–CO bond (CO evolution) and formation of a thermally labile Ru–CHO bond. Besides further reduction of the latter to Ru–CH<sub>2</sub>OH as precursors to CH<sub>3</sub>OH and HOOCCH<sub>2</sub>OH, Ru–CHO reacts with CO<sub>2</sub> to afford HCOOH with regenerating Ru–CO as the precursor to CO. Thus, the difficulty of multi-electron reduction of CO<sub>2</sub> in protic solutions is ascribed to the thermal lability and strong hydride donor character of Ru–CHO. On the other hand, two-electron reduction of Ru–CO in the presence of (CH<sub>3</sub>)<sub>4</sub>N<sup>+</sup> or CH<sub>3</sub>I under aprotic conditions produces thermally stable R–C(O)CH<sub>3</sub>, which works as a precursor to CH<sub>3</sub>C(O)CH<sub>3</sub>. Two-electron reduction of M<sub>3</sub>( $\mu_3$ -S)<sub>2</sub> clusters (M = Co, Rh, Ir) causes an M–M bond cleavage and the nucleophilicity of the  $\mu_3$ -S ligand is also enhanced. As a result, two CO<sub>2</sub> molecules reductively activated probably on  $\mu_3$ -S and metal sites undergo the coupling reaction to give oxalate selectively.

Much attention has been paid to the utilization of CO<sub>2</sub> as a C1 source for chemicals and fuels to cope with an increase in the concentration in air and the oil shortage predicted for the near future. Carbon dioxide behaves as an electrophile under normal conditions. It is well known that CO<sub>2</sub> smoothly inserts into metal–alkyl and –aryl (M–R) bonds to form the corresponding M–OC(O)R complexes as precursors to carboxylic acids.<sup>1)</sup> Dienes and alkynes coordinated to metals are also likely to undergo an electrophilic attack of CO<sub>2</sub> to give lactones and pyrones.<sup>2)</sup> In contrast to such electrophilic attack of CO<sub>2</sub> to organic substrates activated on metals, incorporation of CO<sub>2</sub> activated on metals to relatively inert organic substrates still remains unusual in organic syntheses. Carbon dioxide usually binds to low valent of metals with an  $\eta^1$ - or  $\eta^2$ -mode, where the electron density of the CO<sub>2</sub> group is greatly enhanced due to back electron transfer from the metal to CO<sub>2</sub>. The  $\eta^1$ -CO<sub>2</sub> mode is composed of electron transfer from the filled d<sub>z<sup>2</sup></sub> orbital of d<sup>8</sup> metal centers to the CO<sub>2</sub>  $\pi^*$  orbital, and the  $\eta^2$ -CO<sub>2</sub> mode involves electron transfer from a filled CO<sub>2</sub>  $\pi$  to metal in addition to that from a filled metal  $\pi d$  to the empty CO<sub>2</sub>  $\pi^*$  orbital. The first metal CO<sub>2</sub> complex (M–CO<sub>2</sub>) was Ni(PCy<sub>3</sub>)<sub>2</sub>( $\eta^2$ -CO<sub>2</sub>) prepared by Aresta et al. in 1975.<sup>3)</sup> Since then, a variety of metal complexes with  $\eta^1$ - $\eta^2$ -,  $\mu^2$ -, and  $\mu^3$ -CO<sub>2</sub> modes have been prepared.<sup>4)</sup> Most M– $\eta^1$ -CO<sub>2</sub> complexes are thermally labile and are easily oxidized by air. A C–O bond of M– $\eta^1$ -CO<sub>2</sub> complexes is easily cleaved either by protonation in protic

media or by oxide transfer to free CO<sub>2</sub> in aprotic media, while such transformation from M– $\eta^2$ -CO<sub>2</sub> to M–CO has not been demonstrated so far. Accordingly, CO evolution in electro- and photochemical reduction of CO<sub>2</sub> catalyzed by metal complexes has been simply explained by M– $\eta^1$ -CO<sub>2</sub> intermediates, but little direct evidence has been obtained. One of the most crucial problems in electro- and photochemical reduction of CO<sub>2</sub> using homogeneous catalysts is why the products are limited to only CO and/or HCOOH.<sup>5)</sup> Elucidation of the problem would greatly contribute to constructing a catalytic system that enables multi-electron reduction of CO<sub>2</sub> with forming new carbon–carbon bonds near the equilibrium potentials of the reactions.

A key question for the formation of M– $\eta^1$ -CO<sub>2</sub> complexes how to create coordinatively unsaturated low valent metal centers under mild conditions. On the other hand, adduct formation between CO<sub>2</sub> and organic bases is generally much easier than the formation of M– $\eta^1$ -CO<sub>2</sub> ones. The OCO angle of both adducts probably depends on the number of electrons transferred to the CO<sub>2</sub> moieties. The linear OCO of free CO<sub>2</sub> is hardly influenced at all by adduct formation with a weak base such as NH<sub>3</sub>CO<sub>2</sub>. On the other hand, the

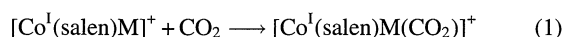
OCO angle of the imidazolidone–CO<sub>2</sub> adduct (OOC–NC(O)–NHCH<sub>2</sub>CH<sub>2</sub>)<sup>–</sup> is calculated as 132°,<sup>6)</sup> which is quite close to those of [Co(Pr-salen)K( $\eta^1$ -CO<sub>2</sub>)] (132°) and [Rh(diars)-

$2(\eta^1\text{-CO}_2)]$  ( $126^\circ$ ).<sup>7)</sup> Thus,  $\text{CO}_2$  bonded to strong organic bases is also reductively activated similar to the process on low valent metals. A fundamental difference in the reductive activation of  $\text{CO}_2$  on metals and organic bases is that the  $\text{CO}_2/\text{CO}$  conversion takes place on the former, but practically does not on the latter. Reductive activation of  $\text{CO}_2$  on organic bases, therefore, may be utilized in  $\text{CO}_2$  fixation without any accompanying C–O bond cleavage. It is worthy of note that acidity and basicity of neighboring groups (ligands) of the central metals are largely influenced by redox reactions of metal complexes even if the reactions are simply explained by the change of oxidation numbers of the central metals. Accordingly, basic ligands as well as metals are possible binding sites for the reductive activation of  $\text{CO}_2$ , and the reactivity of the activated  $\text{CO}_2$  on both sites are regulated by the redox reaction of the metal complexes.

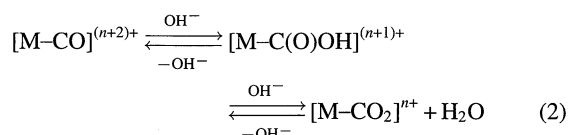
This article focuses on activation of  $\text{CO}_2$  on metals and ligands directed toward multi-electron reduction of  $\text{CO}_2$  accompanied by carbon–carbon bond formation in the electrochemical reduction of  $\text{CO}_2$  catalyzed by metal complexes.

### Metal– $\eta^1\text{-CO}_2$ Complexes

The first  $\text{M-}\eta^1\text{-CO}_2$  ( $\text{M}$  = transition metal) complex was prepared by the reaction of  $\text{CO}_2$  with  $[\text{Co}^{\text{I}}(\text{salen})\text{M}]^+$  ( $\text{M}=\text{Li, Na, K, and Cs}$ ), where alkali metals used for the reduction of  $[\text{Co}^{\text{II}}(\text{salen})]$  remains in the  $\text{Co-}\eta^1\text{-CO}_2$  adducts and strongly interacts with oxygen of  $\text{CO}_2$  binding to  $\text{Co}(\text{I})$  (Eq. 1).<sup>7a)</sup>

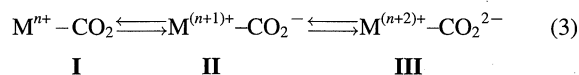


Since then, a series of the  $\text{Co}^{\text{I}}\text{-}\eta^1\text{-CO}_2$  complexes with Schiff bases and macrocyclic ligands have been characterized.<sup>8)</sup> The electron donor ability of the central metal atoms gives crucial influences on the stability of the  $\text{M-}\eta^1\text{-CO}_2$  bond. In fact,  $\text{Co}(\text{I})$  complexes with the redox potential of the  $\text{Co}(\text{I})/\text{Co}(\text{II})$  couple more positive than  $-1.2$  V essentially lose the ability to bind  $\text{CO}_2$  at room temperature.<sup>9)</sup> Similar to  $\text{Co}^{\text{I}}\text{-}\eta^1\text{-CO}_2$  complexes, anionic  $[\text{CpM}(\text{CO})_2(\eta^1\text{-CO}_2)]^-$  ( $\text{M}=\text{Fe, Ru}$ )<sup>10)</sup> and  $[\text{W}(\text{CO})_5(\eta^1\text{-CO}_2)]^{2-}$ <sup>11)</sup> were prepared by the reaction of  $[\text{CpM}(\text{CO})_2]^-$  and  $[\text{W}(\text{CO})_5]^{2-}$  with  $\text{CO}_2$  at low temperatures. Neutral  $\text{Rh-}$  and  $\text{Ir-}\eta^1\text{-CO}_2$  complexes are prepared by an electrophilic attack of  $\text{CO}_2$  to penta-coordinated  $[\text{Ir}^{\text{I}}\text{Cl}(\text{dmpe})_2]^{12)}$  and  $[\text{Rh}^{\text{I}}\text{Cl}(\text{diars})_2]^{7b)}$ . Another synthetic route for  $\text{M-}\eta^1\text{-CO}_2$  complexes is deprotonation of  $\text{M-C(O)OH}$  complexes derived from a nucleophilic attack of  $\text{OH}^-$  (or  $\text{H}_2\text{O}$ ) to carbonyl carbon of electron deficient  $\text{M-CO}$  complexes (Eq. 2).



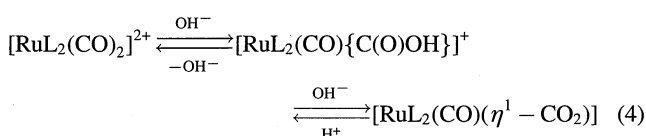
As  $\text{M-}\eta^1\text{-CO}_2$  complexes are generally not stable in  $\text{H}_2\text{O}$ , only a series of  $[\text{Ru}(\text{bpy})_2(\text{CO})(\eta^1\text{-CO}_2)]$ ,  $[\text{Ru}(\text{bpy})_2(\text{CO})\{\text{C(O)OH}\}]^+$ , and  $[\text{Ru}(\text{bpy})_2(\text{CO})_2]^{2+}$  have been shown to exist as equilibrium mixtures in  $\text{H}_2\text{O}$  (see below).<sup>13)</sup> A general tendency for the relative stability of  $\text{M-C-}$

$(\text{O})\text{OH}$  and  $\text{M-}\eta^1\text{-CO}_2$  complexes is not clear, because  $[\text{FeCp}(\text{PPh}_3)(\text{CO})\{\text{C(O)OH}\}]$  loses  $\text{CO}_2$  faster than  $[\text{FeCp}(\text{PPh}_3)(\text{CO})(\eta^1\text{-CO}_2)]^-$ ,<sup>14)</sup> but the reverse is true for  $[\text{ReCp}(\text{NO})(\text{CO})\{\text{C(O)OH}\}]^{15)}$  and  $[\text{IrCl}_2(\text{PMe}_2\text{Ph})_2(\text{CO})\{\text{C(O)OH}\}]^{16)}$ . The basicity of an  $\eta^1\text{-CO}_2$  group, that has a fundamental importance to understand the reactivity of the  $\text{M-}\eta^1\text{-CO}_2$  complexes, can be reasonably evaluated from the conjugated acids,  $\text{M-C(O)OH}$  complexes. In contrast to  $\text{pK}_a$  values of organic carboxylic acids, the values of  $\text{M-C(O)OH}$  complexes widely range from ca. 2 to over 14 (Table 1) due to a large difference in the electron donor ability of the central metals to the  $\text{CO}_2$  group. Despite such large differences in the basicity of  $\text{M-}\eta^1\text{-CO}_2$  complexes, the knowledge concerning the structures and the basicity of  $\eta^1\text{-CO}_2$  group is quite limited, since only three  $\text{M-}\eta^1\text{-CO}_2$  complexes have had their molecular structures determined X-ray analysis so far. The electronic states of  $\text{M-}\eta^1\text{-CO}_2$  complexes would be represented by resonance forms of I, II, and III (Eq. 3).



The amounts of electrons transferred to  $\text{CO}_2$  increased in the order  $\text{I} < \text{II} < \text{III}$ , and the  $\text{M-CO}_2$  bond will be strengthened in the same order. The alkaline metal ( $\text{M}'$ ) as a counter ion of  $[\text{Co}^{\text{I}}(\text{salen})\text{M}'(\eta^1\text{-CO}_2)]^+$  (Eq. 1) which strongly interacts with oxygen of the  $\text{CO}_2$  group must assist the electron flow from  $\text{Co}^{\text{I}}$  to  $\text{CO}_2$  to stabilize the  $\text{Co-}\eta^1\text{-CO}_2$  bond.

An addition of 2 equiv of  $\text{OH}^-$  to an  $\text{H}_2\text{O}/\text{CH}_3\text{OH}$  solution of  $[\text{RuL}_2(\text{CO})_2]^{2+}$  ( $\text{L}=2,2'$ -bipyridine) crystallizes red  $[\text{RuL}_2(\text{CO})(\eta^1\text{-CO}_2)] \cdot 3\text{H}_2\text{O}$ ; this complex is exceptionally stable among those metal– $\eta^1\text{-CO}_2$  complexes reported so far. The interconversion among  $\text{cis-}[\text{RuL}_2(\text{CO})_2]^{2+}$ ,  $\text{cis-}[\text{RuL}_2(\text{CO})\{\text{C(O)OH}\}]^+$  and  $\text{cis-}[\text{RuL}_2(\text{CO})(\eta^1\text{-CO}_2)]$  in  $\text{H}_2\text{O}$  is very rapid (Eq. 4) and  $\text{pK}_a$  of  $[\text{RuL}_2(\text{CO})\{\text{C(O)OH}\}]^+$  is determined as 9.6 at  $20^\circ\text{C}$ .<sup>13)</sup>



Molecular structures of the three complexes are determined by X-ray analysis.<sup>17,18)</sup> The framework of the *trans*- $\text{N-Ru-CO}$ , *trans*- $\text{N-Ru-C(O)OH}$ , and *trans*- $\text{N-Ru-CO}_2$  moieties of  $[\text{RuL}_2(\text{CO})_2](\text{PF}_6)_2$ ,  $[\text{RuL}_2(\text{CO})(\text{C(O)OH})] \cdot (\text{H}_2\text{O})\text{CF}_3\text{COO}$ , and  $[\text{RuL}_2(\text{CO})(\eta^1\text{-CO}_2)] \cdot 3\text{H}_2\text{O}$ , respectively, are depicted in Fig. 1. Red crystals of  $[\text{RuL}_2(\text{CO})(\eta^1\text{-CO}_2)] \cdot 3\text{H}_2\text{O}$  contain three-dimensional hydrogen bonding

Table 1.  $\text{pK}_a$  Values of Hydroxycarbonyl Metal Complexes

Complex	$\text{pK}_a$	Ref.
$\text{ReCp}(\text{NO})(\text{CO})(\text{CO}_2\text{H})$	11	15
$[\text{RuL}_2(\text{CO})(\text{CO}_2\text{H})]^+$	9.6	13
$\text{Pt}(\text{C}_6\text{H}_5)(\text{PEt}_3)(\text{CO}_2\text{H})$	14	19
$[\text{CoL}(\text{CO}_2\text{H})]^{2+}$	3.1	8d
$[\text{Co}(\text{en})_2(\text{H}_2\text{O})(\text{CO}_2\text{H})]^{2+}$	2.5	8e

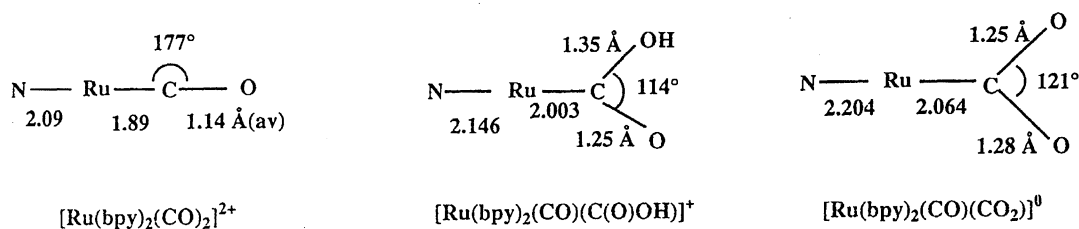


Fig. 1. *trans*-N-Ru-C frameworks of  $[\text{RuL}_2\text{X}(\text{CO})]^{2+}$ ,  $[\text{RuL}_2\text{X}(\text{C}(\text{O})\text{OH})]^+$ , and  $[\text{RuL}_2\text{X}(\text{CO}_2)]$  (L=bpy; X=CO).

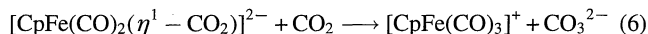
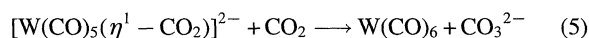
networks among two oxygens of the  $\eta^1$ -CO<sub>2</sub> ligand and three hydrate molecules, which must assist electron flow to the CO<sub>2</sub> group from Ru and stabilizes the Ru-CO<sub>2</sub> bond. Nonequivalent two C-O bond distances (1.25 and 1.28 Å) of the  $\eta^1$ -CO<sub>2</sub> group, therefore, are caused by the differences in the number of hydrogen bondings between the two oxygen and hydrate water molecules. The Ru-CO<sub>2</sub> bond distance (2.06 Å) is close to that of  $[\text{RhCl}(\text{diars})_2(\eta^1\text{-CO}_2)]$  (2.05 Å)<sup>7b)</sup> but longer than of  $[\text{Co}(\text{Pr-salen})(\text{K})(\eta^1\text{-CO}_2)]$  (1.99 Å).<sup>7a)</sup> The average of the C-O bond distance in the  $\eta^1$ -CO<sub>2</sub> group (1.27 Å) is somewhat longer than the average of the C-O ones (1.23 Å) of  $[\text{RhCl}(\text{diars})_2(\eta^1\text{-CO}_2)]$  and  $[\text{Co}(\text{Pr-salen})(\text{K})(\eta^1\text{-CO}_2)]$ . The OCO angle (121°) of the Ru-CO<sub>2</sub> group is narrower than those of Rh- $\eta^1$ -CO<sub>2</sub> (126°) and Co- $\eta^1$ -CO<sub>2</sub> (135°). The C-O bond distance and the OCO angle of CO<sub>2</sub><sup>-</sup> are calculated as 1.24 Å and 135.2°, respectively, by ab initio MO calculations.<sup>19)</sup> If an OCO angle of metal- $\eta^1$ -CO<sub>2</sub> complexes is correlated with the amount of electrons transferred to the CO<sub>2</sub> ligands,  $\sigma$ -donation from Ru to CO<sub>2</sub> is stronger than that from Co and Rh to CO<sub>2</sub>. Based on the p*K*<sub>a</sub> values of Ru-C(O)OH (9.6) and Co- $\eta^1$ -C(O)OH complexes (2–3) (Table 1), and the OCO angles of  $[\text{RuL}_2(\text{CO})(\eta^1\text{-CO}_2)]$  (121°),  $[\text{Co}(\text{Pr-salen})(\text{K})(\eta^1\text{-CO}_2)]$  (135°),<sup>17)</sup> and CO<sub>2</sub><sup>-</sup> (135°), the electronic states of the Ru- and Co- $\eta^1$ -CO<sub>2</sub> complexes are approximated by the resonance forms III and II, respectively. Accordingly,  $[\text{RhCl}(\text{diars})_2(\eta^1\text{-CO}_2)]^{7b)}$  may be expressed by an intermediate between the resonance forms II and III on the basis of the OCO angle, though the p*K*<sub>a</sub> value of the conjugated acid is not clear.

The relatively high electron density on the CO<sub>2</sub> group of  $[\text{RuL}_2(\text{CO})(\eta^1\text{-CO}_2)]$  is responsible for the smooth transformation from CO<sub>2</sub> to CO on the Ru atom in H<sub>2</sub>O. The C=O and C-O bond distances (1.242 and 1.345 Å) and the OCO angle of 119° of  $[\text{RuL}_2(\text{CO})(\text{C}(\text{O})\text{OH})]^+$  are close to the values of  $[\text{Pt}(\text{C}_6\text{H}_5)(\text{PET}_3)_2\{\text{C}(\text{O})\text{OH}\}]$ ,<sup>19)</sup> which exists as a hydrogen-bonded dimer structure similar to the solid state of acetic acid. Protonation of the CO<sub>2</sub> group of  $[\text{RuL}_2(\text{CO})(\eta^1\text{-CO}_2)]$  causes shortening both the Ru- $\eta^1$ -CO<sub>2</sub> and the Ru-N (*trans* to Ru-CO<sub>2</sub>) bonds. Dehydroxylation of  $[\text{RuL}_2(\text{CO})\{\text{C}(\text{O})\text{OH}\}]^+$  further shortens the Ru-C and Ru-N (*trans* to Ru-C(O)OH) bonds (Fig. 1). The Ru- $\eta^1$ -CO<sub>2</sub> bond is primarily composed of  $\sigma$ -donation from Ru to CO<sub>2</sub>, and the Ru-CO bond consists of  $\pi$ -back donation from Ru to CO and weak  $\sigma$ -donation from CO to Ru. The gradual elongation of the Ru-C bond distances from Ru-CO, Ru-C(O)OH to Ru-CO<sub>2</sub>, therefore, strongly reflects the decrease in the  $\pi$ -bonding rather than the increase in the  $\sigma$ -bonding in the Ru-C bonds. It is worthy of note that an increase in the  $\sigma$ -donation from metals

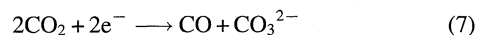
to CO<sub>2</sub> strengthens M- $\eta^1$ -CO<sub>2</sub> bonds, but does not always shorten the Ru-C bond distances. The agreement of the order of the Ru-CO < Ru-C(O)OH < Ru-CO<sub>2</sub> bond distances with *trans*-Ru-N ones strongly indicates that bpy as a  $\sigma$ -donor and  $\pi$ -acceptor ligand plays a role as an electron reservoir in the serious changes in the electronic structures of Ru in the equilibrium of Eq. 4. It should be noticed that  $[\text{RuL}_2(\text{CO})(\eta^1\text{-CO}_2)]$  does not undergo a serious change at 100 °C in H<sub>2</sub>O at pH 11 for 3 h, while  $[\text{CpRu}(\text{CO})_2(\eta^1\text{-CO}_2)]\text{Na}$  decomposes to  $[\text{CpRu}(\text{CO})_2(\text{H})]$  in THF at 0 °C.<sup>20)</sup> Thus, bpy ligands greatly contribute to the exceptional thermal stability of  $[\text{RuL}_2(\text{CO})(\eta^1\text{-CO}_2)]$  as a metal- $\eta^1$ -CO<sub>2</sub> complex.

#### Conversion from M-CO<sub>2</sub> to M-CO under Aprotic Conditions

Anionic  $[\text{CpFe}(\text{CO})_2(\eta^1\text{-CO}_2)]^-$  and  $[\text{W}(\text{CO})_5(\eta^1\text{-CO}_2)]^{2-}$  smoothly react with CO<sub>2</sub> to produce  $[\text{CpFe}^I(\text{CO})_3]^+$  and  $[\text{W}^0(\text{CO})_6]$ , respectively, with forming CO<sub>3</sub><sup>2-</sup> (Eqs. 5 and 6).<sup>20a,20b)</sup>



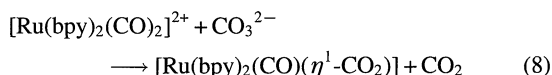
Thus,  $[\text{M}-\eta^1\text{-CO}_2]^{n+}$  with a very strong basic CO<sub>2</sub> group undergoes the oxide transfer reaction by free CO<sub>2</sub> to generate CO<sub>3</sub><sup>2-</sup> and  $[\text{M-CO}]^{(n+2)+}$ , the latter of which works as the precursor to CO in electrochemical reduction of CO<sub>2</sub> (reductive disproportionation of CO<sub>2</sub>) under aprotic conditions (Eq. 7).



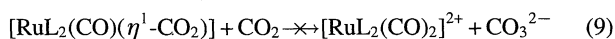
But no oxide transfer reaction from CO<sub>3</sub><sup>2-</sup> to M-CO complexes (reverse reaction of Eqs. 5 and 6) has been reported so far. Comparison of the basicity of M- $\eta^1$ -CO<sub>2</sub> and CO<sub>3</sub><sup>2-</sup> as oxide donors would greatly help us to understand the differences in the two bonds on the basis of p*K*<sub>a</sub> values of the conjugated acids:  $[\text{Ru}(\text{bpy})_2(\text{CO})\{\text{C}(\text{O})\text{OH}\}]^+$  (9.6)<sup>7)</sup> and HOCO<sub>2</sub><sup>-</sup> (10.3).<sup>22)</sup> Red crystals of  $[\text{RuL}_2(\text{CO})(\eta^1\text{-CO}_2)] \cdot 3\text{H}_2\text{O}$  are soluble only in protic media such as H<sub>2</sub>O, CH<sub>3</sub>OH, C<sub>2</sub>H<sub>5</sub>OH, but are insoluble in aprotic solvents. The characteristic solubility of the red crystals in both media is explained by the three dimensional hydrogen bonding networks of solvated water molecules in the solid state. On the other hand, the red crystals are smoothly solubilized into a CH<sub>3</sub>CN solution containing LiCF<sub>3</sub>SO<sub>3</sub> due to destruction of 3-dimensional hydrogen bonding networks of  $[\text{RuL}(\text{CO})(\text{CO}_2)] \cdot 3\text{H}_2\text{O}$  by interaction of Li<sup>+</sup> with oxygens of the  $\eta^1$ -CO<sub>2</sub> group.

The IR spectrum of a CD<sub>3</sub>CN solution containing [RuL(CO)(CO<sub>2</sub>)]·3H<sub>2</sub>O and 3 equiv of LiCF<sub>3</sub>SO<sub>3</sub> showed strong  $\nu_{\text{asym}}(\text{CO}_2)$  and  $\nu_{\text{sym}}(\text{CO}_2)$  bands at 1467 and 1246 cm<sup>-1</sup>, which are close those of [RuL<sub>2</sub>(CO)( $\eta^1$ -CO<sub>2</sub>)]·3H<sub>2</sub>O in KBr disks (1428 and 1242 cm<sup>-1</sup>).<sup>17)</sup> Thus, the molecular structure of [RuL<sub>2</sub>(CO)( $\eta^1$ -CO<sub>2</sub>)]·3H<sub>2</sub>O in the solid state is maintained also in CH<sub>3</sub>CN containing LiCF<sub>3</sub>SO<sub>3</sub>. Solubilization of [RuL<sub>2</sub>(CO)( $\eta^1$ -CO<sub>2</sub>)] in aprotic media enabled the direct interconversion between [RuL<sub>2</sub>(CO)( $\eta^1$ -CO<sub>2</sub>)] and [RuL<sub>2</sub>(CO)<sub>2</sub>]<sup>2+</sup> without passing through [RuL<sub>2</sub>(CO){C(O)OH}]<sup>+</sup>. Similarly, we found that [RuL<sub>2</sub>(CO)( $\eta^1$ -CO<sub>2</sub>)] is solubilized in CH<sub>3</sub>CN in the presence of [K(crown)]<sup>+</sup>.

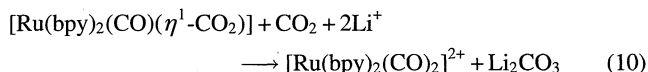
The reaction of [K(crown)]<sub>2</sub>CO<sub>3</sub> with [RuL<sub>2</sub>(CO)<sub>2</sub>](PF<sub>6</sub>)<sub>2</sub> afforded [RuL<sub>2</sub>(CO)( $\eta^1$ -CO<sub>2</sub>)] and CO<sub>2</sub> in CH<sub>3</sub>CN (Eq. 8).<sup>21)</sup>



Thus, the reaction of Eq. 8 is the first example of the oxide transfer from CO<sub>3</sub><sup>2-</sup> to M-CO, and the resultant [Ru(bpy)<sub>2</sub>(CO)( $\eta^1$ -CO<sub>2</sub>)] remained unchanged even after CO<sub>2</sub> bubbling into the solution (Eq. 9).



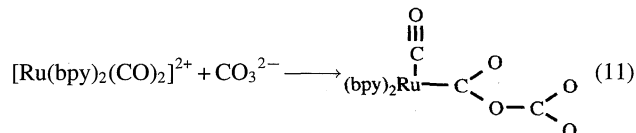
Moreover, the reaction of [RuL<sub>2</sub>(<sup>12</sup>CO)(<sup>13</sup>CO)]<sup>2+</sup> with [K(crown)]<sub>2</sub><sup>12</sup>CO<sub>3</sub> evolved only <sup>12</sup>CO<sub>2</sub> in CH<sub>3</sub>CN. On the other hand, an addition of LiCF<sub>3</sub>SO<sub>3</sub> to the CO<sub>2</sub>-saturated CH<sub>3</sub>CN solution containing [RuL<sub>2</sub>(CO)( $\eta^1$ -CO<sub>2</sub>)] resulted in gradual precipitation of Li<sub>2</sub>CO<sub>3</sub> with the generation of [RuL<sub>2</sub>(CO)<sub>2</sub>]<sup>2+</sup> (Eq. 10).



Thus, removal of CO<sub>3</sub><sup>2-</sup> from the solution as a precipitation forced the oxide transfer from [RuL<sub>2</sub>(CO)( $\eta^1$ -CO<sub>2</sub>)] to CO<sub>2</sub> to take place in CH<sub>3</sub>CN. The interaction of Li<sup>+</sup> with the  $\eta^1$ -CO<sub>2</sub> would induce the electron transfer from Ru to CO<sub>2</sub>, which results in an increase of nucleophilicity of the CO<sub>2</sub> ligand to lead to the formation of CO<sub>3</sub><sup>2-</sup>. It is worthy of note that the oxide transfer from [K(crown)]<sub>2</sub>CO<sub>3</sub> to [RuL<sub>2</sub>(CO)<sub>2</sub>]<sup>2+</sup> in CH<sub>3</sub>CN (Eq. 8) finished in a few minutes, while it took an almost one day to complete the reverse reaction in the presence of LiCF<sub>3</sub>SO<sub>3</sub> in CO<sub>2</sub>-saturated CH<sub>3</sub>CN (Eq. 10).

The rate of the oxide transfer reaction from [(CH<sub>3</sub>)<sub>4</sub>N]<sub>2</sub>CO<sub>3</sub> to [RuL<sub>2</sub>(CO)<sub>2</sub>]<sup>2+</sup> in DMSO is slow and the reaction intermediate was detected by the <sup>13</sup>C NMR spectra. The <sup>13</sup>C NMR spectra of a d<sub>6</sub>-DMSO solution right after

mixing [RuL<sub>2</sub>(<sup>12</sup>CO)(<sup>13</sup>CO)](PF<sub>6</sub>)<sub>2</sub> and [(CH<sub>3</sub>)<sub>4</sub>N]<sub>2</sub>CO<sub>3</sub> displayed two signals at  $\delta$ =201.7 and 205.2 ppm. The chemical shifts of these signals are almost identical with those of [RuL<sub>2</sub>(CO){C(O)OH}]<sup>+</sup> in DMSO, suggesting the formation of a 1:1 adduct by an attack of CO<sub>3</sub><sup>2-</sup> to a carbonyl carbon of [RuL<sub>2</sub>(CO)<sub>2</sub>]<sup>2+</sup> (Eq. 11).

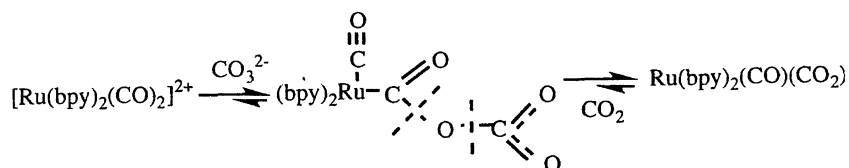


The fission of either the RuCO<sub>2</sub>-CO<sub>2</sub> or RuC(O)-CO<sub>3</sub> bond of the 1:1 adduct determines the direction of the oxide transfer reactions of Eqs. 8, 9, and 10 (Scheme 1). The unusual oxide transfer reaction of Eq. 8 via the RuC(O)O-CO<sub>2</sub> bond fission (Scheme 1) is interpreted as the conversion from a weak base (CO<sub>3</sub><sup>2-</sup>) to a weaker one ([RuL<sub>2</sub>(CO)( $\eta^1$ -CO<sub>2</sub>)]). Although the oxide transfer reaction of Scheme 1 lies so far to [RuL<sub>2</sub>(CO)( $\eta^1$ -CO<sub>2</sub>)], the shift to [RuL<sub>2</sub>(CO)<sub>2</sub>]<sup>2+</sup> in the equilibrium by an addition of Li<sup>+</sup> indicates the small energy difference in the formation of the two complexes.

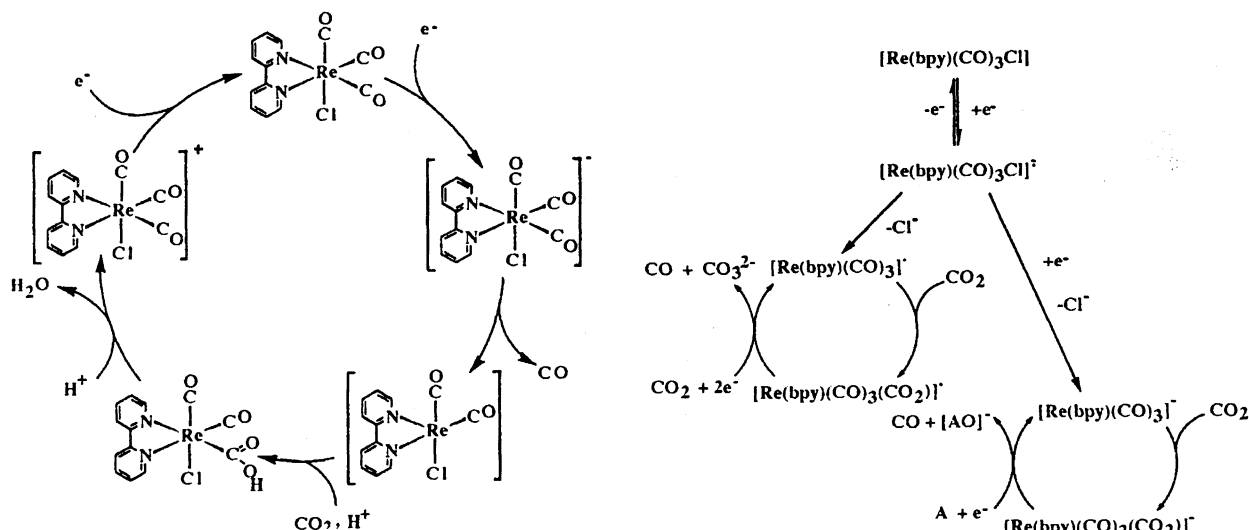
### Electrochemical Reduction of CO<sub>2</sub> Catalyzed by Metal Complexes

A large number of metal complexes have proven to be active as catalysts precursors in electro- and photochemical reduction of CO<sub>2</sub>.<sup>5)</sup> Among those metal complexes, three metal complexes: [ReCl(L)(CO)<sub>3</sub>], [Ni(cyclam)]<sup>2+</sup> and [RuL<sub>2</sub>(CO)<sub>2</sub>]<sup>2+</sup>, have attracted much attention because of their characteristic reactivity and high efficiency in the reduction of CO<sub>2</sub>.

Lehn et al. reported electrochemical reduction of CO<sub>2</sub> catalyzed by [ReCl(L)(CO)<sub>3</sub>] in 1984.<sup>23)</sup> A series of [ReCl(L)-(L')(CO)<sub>2</sub>] (L'=neutral ligand) have bifunctional ability as photosensitizers and as catalysts in the photochemical reduction of CO<sub>2</sub> to CO. Since they proposed a reaction mechanism for CO evolution in 1986 (Scheme 2), the arguments concerning the reaction mechanisms have still continued because no reasonable reaction intermediate has been characterized.<sup>24)</sup> The main arguments are i) whether Cl<sup>-</sup> or CO initially dissociates from one-electron reduced form, ii) whether another one-electron reduction takes place or not before the resultant five-coordinate (or solvated) Re complex undergoes an electrophilic attack of CO<sub>2</sub>. A recent IR spectroelectrochemical study suggests the occurrence of the CO<sub>2</sub> attack to both [ReL(CO)<sub>3</sub>]<sup>-</sup> (two electron reduced form) and [Re(dmbpy)(CO)<sub>3</sub>]<sup>-</sup> (one electron reduced form) (dmbpy=4,4'-dimethyl-2,2'-bipyridine) depending on their stability under electrolysis conditions.<sup>25)</sup>



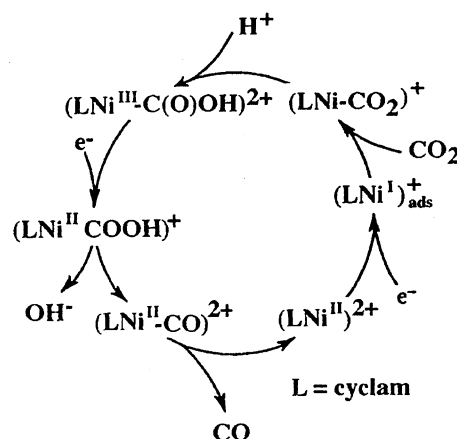
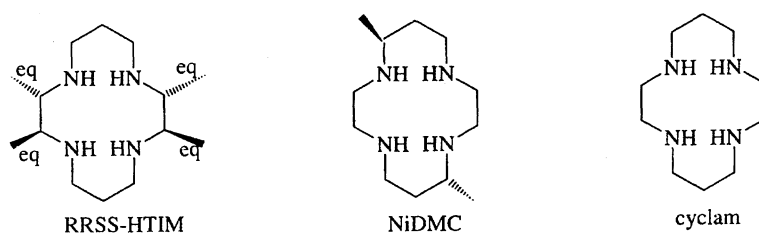
Scheme 1. The first reversible oxide transfer through a metal-C(O)-O-CO<sub>2</sub> adduct.

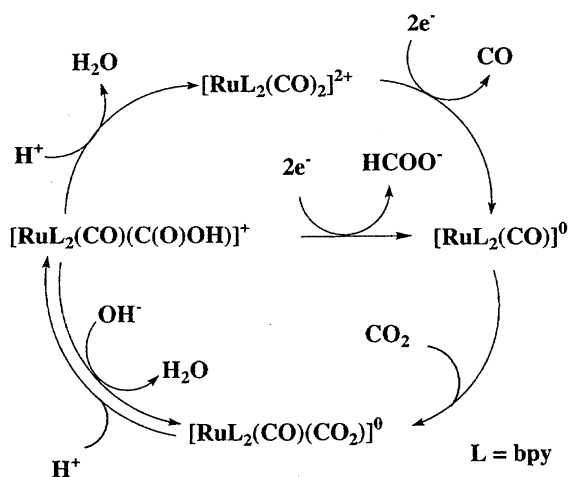
Scheme 2. Proposed mechanisms for the electrochemical reduction of CO<sub>2</sub> catalyzed by [Re(bpy)(CO)<sub>3</sub>Cl].

Sauvage et al. found [Ni(cyclam)]<sup>2+</sup> adsorbed on an Hg electrode evolves CO with an almost 100% current efficiency in the electrochemical reduction of CO<sub>2</sub> in H<sub>2</sub>O.<sup>29)</sup> The reaction is explained by Scheme 3, though none of Ni-CO<sub>2</sub>, -C(O)OH or -CO species have been identified. Sakaki et al. reported SCF ab initio calculations for [NiF(NH<sub>3</sub>)<sub>4</sub>]<sup>+</sup> as the model of [Ni(cyclam)]<sup>+</sup> adsorbed on Hg, and proposed a Ni<sup>I</sup>-η<sup>1</sup>-CO<sub>2</sub> adduct with the Ni-C bond distance of 1.92 Å and the OCO angle of 135.3° as the active species for the CO<sub>2</sub> reduction.<sup>30)</sup> The selectivity of CO/H<sub>2</sub> formation in the CO<sub>2</sub> reduction catalyzed by Ni(macrocyclic) complexes largely depends on the substituents of the ligands, and some of the derivatives are more reactive toward the selective CO<sub>2</sub> reduction than [Ni(cyclam)]<sup>2+</sup>.<sup>31)</sup> However, little is known about why [Ni(cyclam)]<sup>2+</sup> adsorbed on the surface of Hg selectively reduces CO<sub>2</sub> in H<sub>2</sub>O via a possible intermediate of the Ni-η<sup>1</sup>-CO<sub>2</sub> complex (Chart 1).

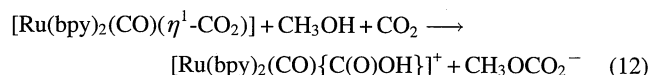
Tanaka et al. reported that electrolysis of [RuL<sub>2</sub>(CO)<sub>2</sub>]<sup>2+</sup> at -1.20 V (vs. SCE) in DMF/H<sub>2</sub>O (1 : 9 v/v, pH 6.0) under CO<sub>2</sub> atmosphere produced CO and H<sub>2</sub>, while the same electrolysis conducted at pH 9.5 gave H<sub>2</sub>, CO, and HCOO<sup>-</sup> with a mole ratio of 1 : 1 : 1 in 1985.<sup>26)</sup> Furthermore, the electrochemical reduction of CO<sub>2</sub> by [RuL<sub>2</sub>(CO)<sub>2</sub>]<sup>2+</sup> in dry CH<sub>3</sub>CN in the presence of Me<sub>3</sub>NHCl as a proton source predominantly produces HCOO<sup>-</sup> with a current efficiency of 85%.<sup>27)</sup> The alternation of the main product from CO to HCOO<sup>-</sup> with decreasing the proton concentrations in the reaction media is correlated with the equilibrium among [RuL<sub>2</sub>(CO)<sub>2</sub>]<sup>2+</sup>,

[RuL<sub>2</sub>(CO){C(O)OH}]<sup>+</sup> and [RuL<sub>2</sub>(CO)(η<sup>1</sup>-CO<sub>2</sub>)]<sup>0</sup> (Eq. 4) in the solution. Moreover, photochemical reduction of CO<sub>2</sub> catalyzed by the [RuL<sub>2</sub>(CO)<sub>2</sub>]<sup>2+</sup>/[RuL<sub>3</sub>]<sup>2+</sup>/N(CH<sub>2</sub>OH)<sub>3</sub> system in dry DMF selectively produces HCOO<sup>-</sup> in a quantum yield (η=14%), while CO becomes the main product (η=14.8%) in the similar CO<sub>2</sub> reduction catalyzed by the [RuL<sub>2</sub>(CO)<sub>2</sub>]<sup>2+</sup>/[RuL<sub>3</sub>]<sup>2+</sup>/BNAH system (BNAH=1-benzyl-1,4-dihydronicotinamide) in DMF/H<sub>2</sub>O mixture.<sup>27)</sup> These facts indicate that the electro- and photochemical reductions of CO<sub>2</sub> catalyzed by [RuL<sub>2</sub>(CO)<sub>2</sub>]<sup>2+</sup> proceed in similar mechanisms. Electrochemical reduction of CO<sub>2</sub> catalyzed by

Scheme 3. Proposed mechanism for the electrochemical reduction of CO<sub>2</sub> by [Ni(cyclam)]<sup>2+</sup>.Chart 1. RRSS-NiHTIM<sup>2+</sup>, NiDMC<sup>2+</sup>, and Nicyclam<sup>2+</sup>.

Scheme 4. Reduction of CO<sub>2</sub> catalyzed by [Ru(bpy)<sub>2</sub>(CO)<sub>2</sub>]<sup>2+</sup>.

[RuL<sub>2</sub>(CO)<sub>2</sub>]<sup>2+</sup> is explained by Scheme 4; [RuL<sub>2</sub>(CO)<sub>2</sub>]<sup>2+</sup> undergoes irreversible two-electron reduction at -1.0 V (vs. SCE) (vide infra) to evolve CO with generating penta-coordinated [RuL<sub>2</sub>(CO)]<sup>0</sup>, which reacts with CO<sub>2</sub> to form [RuL<sub>2</sub>(CO)( $\eta^1$ -CO<sub>2</sub>)]. Protonation of [RuL<sub>2</sub>(CO)( $\eta^1$ -CO<sub>2</sub>)] gives [RuL<sub>2</sub>(CO)<sub>2</sub>]<sup>2+</sup> through [RuL<sub>2</sub>(CO){C(O)OH}]<sup>+</sup>, both of which function as the precursors to CO and HCOO<sup>-</sup> formation. It is worthy of note that [RuL<sub>2</sub>(CO)( $\eta^1$ -CO<sub>2</sub>)] is stable in CH<sub>3</sub>OH as expected from the pK<sub>a</sub> value of 9.6, but the  $\eta^1$ -CO<sub>2</sub> complex is completely protonated to give [RuL<sub>2</sub>(CO){C(O)OH}]<sup>+</sup> under CO<sub>2</sub> in the same solvent due to the exothermic formation of CH<sub>3</sub>OCO<sub>2</sub><sup>-</sup> (Eq. 12).

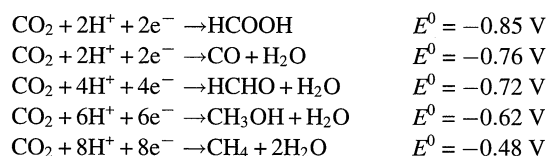


The complete protonation of [Ru(bpy)<sub>2</sub>(CO)( $\eta^1$ -CO<sub>2</sub>)] affording [Ru(bpy)<sub>2</sub>(CO){C(O)OH}]<sup>+</sup> in CH<sub>3</sub>OH under CO<sub>2</sub> (Eq. 12) is, therefore, responsible for the predominant formation of HCOO<sup>-</sup> in the photo- and electrochemical reduction of CO<sub>2</sub> in the presence of weak proton donors. Besides [RuL<sub>2</sub>(CO){C(O)OH}]<sup>+</sup> derived from the equilibrium of Eq. 4, [RuL<sub>2</sub>(CO){OC(O)H}] resulting from CO<sub>2</sub> insertion into the Ru-H bond of [RuL<sub>2</sub>(CO)H]<sup>0</sup> is also suggested as a precursor to HCOO<sup>-</sup> in the reduction of CO<sub>2</sub> catalyzed by [RuL<sub>2</sub>(CO)<sub>2</sub>]<sup>2+</sup>.<sup>28)</sup> Although an intramolecular rearrangement from [RuL<sub>2</sub>(CO){OC(O)H}]<sup>+</sup> to [RuL<sub>2</sub>(CO){C(O)OH}]<sup>+</sup> to explain CO evolution has been also proposed, the conversion between M-OC(O)H and M-C(O)OH has not been demonstrated so far.

### Multi-Electron Reduction of CO<sub>2</sub> under Protic Conditions

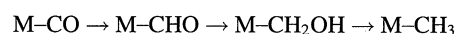
Electro- and photochemical reduction of CO<sub>2</sub> catalyzed by metal complexes under protic conditions generates CO and/or HCOOH together with H<sub>2</sub>. A competitive electrophilic attack of CO<sub>2</sub> and proton to low valent metal centers produces either M-CO<sub>2</sub> or M-H bonds. CO evolution is simply ascribed to a reductive cleavage of a M-CO bond resulting from the acid-base equilibrium of M-CO<sub>2</sub> (Eq. 2).

Besides M-C(O)OH complexes, M-OC(O)H complexes derived from insertion of CO<sub>2</sub> into M-H bonds work as precursors to HCOO<sup>-</sup> generation. The most crucial problem in those CO<sub>2</sub> reductions is why multi-electron reduction of CO<sub>2</sub> with C-C bond formation does not take place in homogeneous reactions. It should be noticed that multi-electron reduction of CO<sub>2</sub> is energetically favored compared with two-electron reduction of CO<sub>2</sub>. The standard redox potentials *E*<sup>0</sup> (vs. SCE) for CO<sub>2</sub> reduction shift to positive potentials (pH 7.0, 20 °C) as the number of electron involved in the reduction increases.

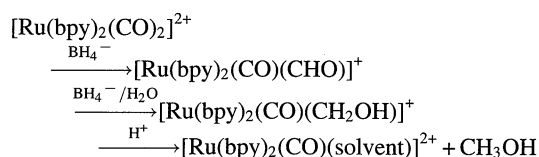


Although general pathways for 4-, 6-, and 8-electron reduction of CO<sub>2</sub> have not been demonstrated so far, the reduction of M-CO rather than M-CO<sub>2</sub> is considered as the key process for multi-electron reduction of CO<sub>2</sub> by considering the smooth transformation between CO<sub>2</sub> and CO on metals. Some of the cationic metal carbonyl complexes are successively reduced to methyl derivatives through formyl-, hydroxymethyl complexes with hydride donors such as NaBH<sub>4</sub> and metal-hydrides (Scheme 5).<sup>33)</sup> As expected from chemical reduction of M-CO to M-CH<sub>3</sub> (Scheme 5), reduction of M-CO to M-CHO prior to M-CO bond cleavage (CO evolution) is likely to be a key step to make the multi-electron reduction of CO<sub>2</sub> in the homogeneous electrochemical reduction.

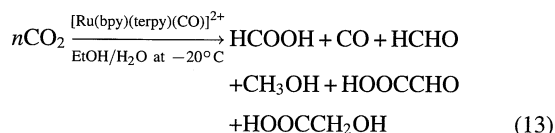
There are great differences in chemical and electrochemical reductions of M-CO complexes: electrochemical reduction of [RuL<sub>2</sub>(CO)<sub>2</sub>]<sup>2+</sup> resulted in a Ru-CO bond cleavage in both protic and aprotic solutions, while a CO group of the complex is reduced to CH<sub>3</sub>OH in a 10% yield by treatments with 4 equiv of NaBH<sub>4</sub> in CH<sub>3</sub>CN/H<sub>2</sub>O. Both [RuL<sub>2</sub>(CO)-(CHO)]<sup>+</sup> and [RuL<sub>2</sub>(CO)(CH<sub>2</sub>OH)]<sup>+</sup> were isolated as the reaction intermediates of CH<sub>3</sub>OH in the same reaction conducted at -20 °C (Scheme 6).<sup>34)</sup> Similarly, treatments of [RuL(terpy)(CO)]<sup>2+</sup> (terpy = 2,2':6',2''-terpyridine) with 4 equiv of BH<sub>4</sub><sup>-</sup> quantitatively produced CH<sub>3</sub>OH and [RuL(terpy)(CH<sub>3</sub>CN)]<sup>+</sup> in the same solvent, where [RuL(terpy)-



Scheme 5. Stepwise reduction of metal-CO complex.

Scheme 6. Reduction of [Ru(bpy)<sub>2</sub>(CO)<sub>2</sub>]<sup>2+</sup> with NaBH<sub>4</sub>.

(CHO)]<sup>+</sup> was initially formed in the same reaction conducted at  $-40^{\circ}\text{C}$ . Despite the formation of  $[\text{RuL}_2(\text{CO})(\text{CHO})]^+$  and  $[\text{RuL}_2(\text{CO})(\text{CH}_2\text{OH})]^+$  as the precursor to  $\text{CH}_3\text{OH}$  in the reaction of  $[\text{RuL}_2(\text{CO})_2]^{2+}$  with  $\text{BH}_4^-$  (Scheme 6), electrochemical reduction of  $\text{CO}_2$  catalyzed by the same complex produced only  $\text{CO}$  and  $\text{HCOOH}$  even at  $-20^{\circ}\text{C}$ . On the other hand, the similar  $\text{CO}_2$  reduction catalyzed by  $[\text{RuL}(\text{terpy})(\text{CO})](\text{PF}_6)_2$  under the same electrolysis conditions produced not only  $\text{CO}$  and  $\text{HCOO}^-$  but also  $\text{HC(O)H}$ ,  $\text{CH}_3\text{OH}$ ,  $\text{H(O)-CCOOH}$ , and  $\text{HOCH}_2\text{COOH}$  (Eq. 13) (Fig. 2).



The difference in the catalytic activity of  $[\text{RuL}(\text{terpy})(\text{CO})]^{2+}$  and  $[\text{RuL}_2(\text{CO})_2]^{2+}$  toward the multi-electron reduction of  $\text{CO}_2$  is associated with the stability of the reduced forms of these complexes at that temperature. Figure 3 shows the cyclic voltammogram (CV) of both complexes in  $\text{CH}_3\text{CN}$  under  $\text{N}_2$  and  $\text{CO}_2$ ;  $[\text{RuL}_2(\text{CO})_2]^{2+}$  undergoes irreversible two-electron reduction at around  $-1.30\text{ V}$  (vs.  $\text{Ag}/\text{Ag}^+$ ) at  $20$  and  $-20^{\circ}\text{C}$ . The CV of  $[\text{RuL}(\text{terpy})(\text{CO})]^{2+}$  displays a reversible redox couples at  $E_{1/2} = -1.37$  and an irreversible cathodic wave at  $-1.69\text{ V}$  at  $20^{\circ}\text{C}$ , while the second redox reaction becomes a reversible electron transfer process at  $-20^{\circ}\text{C}$ . On the basis of the fact that these redox reactions takes place in polypyridyl ligands, the redox behavior of the two complexes (Fig. 3) is explained as follows:  $[\text{Ru}(\text{bpy})-(\text{bpy})(\text{CO})_2]^0$  readily dissociates  $\text{CO}$ , while  $[\text{Ru}(\text{bpy})-(\text{terpy})(\text{CO})]^0$  is stable at  $-20^{\circ}\text{C}$ . Moreover, the reaction

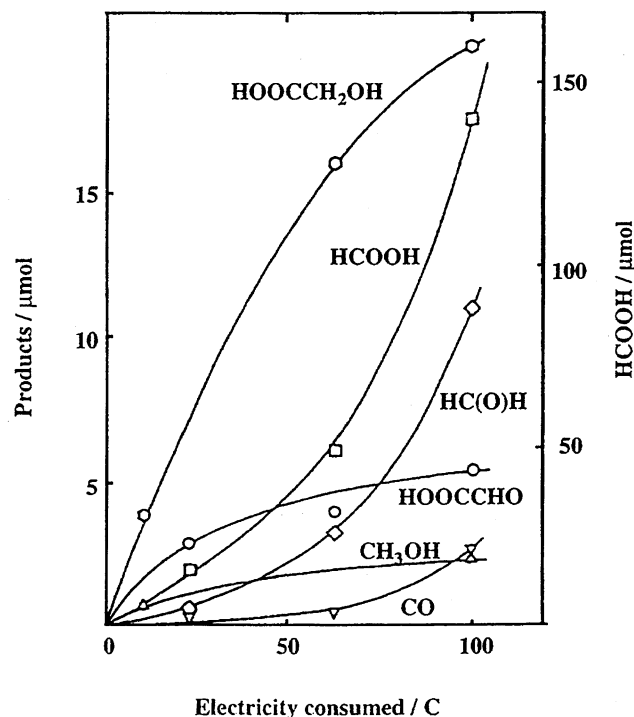


Fig. 2. Multi-electron reduction of  $\text{CO}_2$  catalyzed by  $[\text{Ru}(\text{bpy})(\text{terpy})(\text{CO})]^+$  in  $\text{EtOH}/\text{H}_2\text{O}$  at  $-20^{\circ}\text{C}$ .

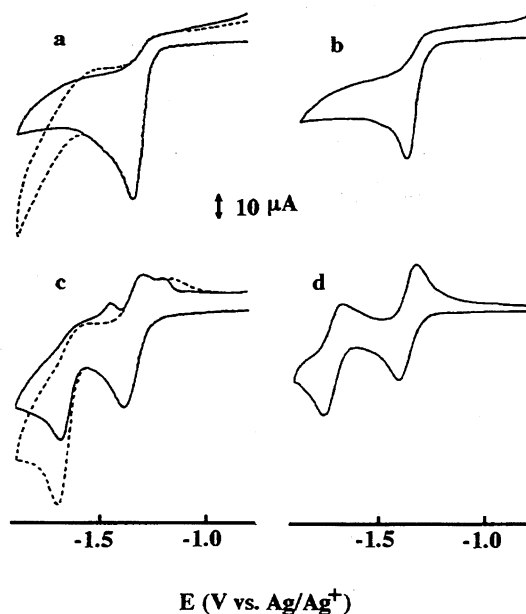
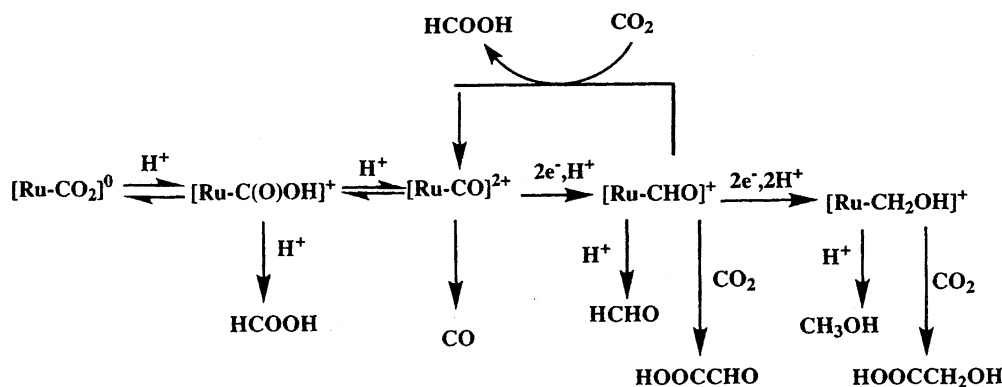


Fig. 3. Cyclic voltammograms of  $[\text{RuL}_2(\text{CO})_2](\text{PF}_6)_2$  (a and b) and  $[\text{RuL}(\text{terpy})(\text{CO})](\text{PF}_6)_2$  (c and d) in  $\text{CH}_3\text{CN}$  at  $20^{\circ}\text{C}$  and  $-20^{\circ}\text{C}$  under  $\text{N}_2$  (solid lines) and  $\text{CO}_2$  (dotted lines).

of  $[\text{RuL}(\text{terpy})(\text{CO})]^0$  with  $\text{H}_2\text{O}$  at  $-30^{\circ}\text{C}$  produced  $[\text{RuL}(\text{terpy})(\text{CHO})]^+$ . Accordingly, the pathway for multi-electron reduction of  $\text{CO}_2$  by  $[\text{RuL}(\text{terpy})(\text{CO})]^{2+}$  is explained by Scheme 7. Transformation from  $[\text{RuL}(\text{terpy})(\text{CO}_2)]^0$  to  $[\text{RuL}(\text{terpy})(\text{CO})]^{2+}$  is ascribed to the acid-base equilibrium of Eq. 2. Two-electron reduction of  $[\text{RuL}(\text{terpy})(\text{CO})]^{2+}$  under protic conditions results in the formation of  $[\text{RuL}(\text{terpy})(\text{CHO})]^+$  and  $\text{CO}$  evolution competitively. Protonation or carboxylation of  $[\text{RuL}(\text{terpy})(\text{CHO})]^+$  under the electrolysis conditions gives  $\text{HCHO}$  and  $\text{HOOCCHO}$ , respectively. Further reduction and protonation of  $[\text{RuL}(\text{terpy})(\text{CHO})]^+$  produces  $[\text{RuL}(\text{terpy})(\text{CH}_2\text{OH})]^+$ , which reacts with proton and  $\text{CO}_2$  to generate  $\text{CH}_3\text{OH}$  and  $\text{HOOCCH}_2\text{OH}$ . It is, however, worthy of note that  $\text{HCOO}^-$  is still formed as the main product in the  $\text{CO}_2$  reduction (Fig. 2), even though the concentration of  $[\text{RuL}(\text{terpy})\{\text{C}(\text{O})\text{OH}\}]^+$  must be negligibly low because of the rapid conversion from  $[\text{RuL}(\text{terpy})(\eta^1\text{-CO}_2)]$  to  $[\text{RuL}(\text{terpy})(\text{CO})]^{2+}$  in  $\text{H}_2\text{O}/\text{C}_2\text{H}_5\text{OH}$ . A trace amount of  $\text{CO}$  evolution also reflects the smooth transformation from  $[\text{RuL}(\text{terpy})(\text{CO}_2)]^0$  to  $[\text{RuL}(\text{terpy})(\text{CHO})]^+$  prior to  $\text{CO}$  dissociation from  $[\text{RuL}(\text{terpy})(\text{CO})]^{2+}$  under the electrolysis conditions. Moreover,  $[\text{RuL}(\text{terpy})(\text{CHO})]^+$ , that was obtained in a stoichiometric reaction of  $\text{LiBEt}_3\text{H}$  with  $[\text{RuL}(\text{terpy})(\text{CO})](\text{PF}_6)_2$  in  $\text{CD}_3\text{CN}$ , smoothly reacts with  $\text{CO}_2$  to produce  $[\text{RuL}(\text{terpy})(\text{CO})]^{2+}$  and  $\text{HCOO}^-$  (60% yield) even at  $-20^{\circ}\text{C}$  (Eq. 14).



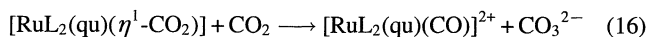
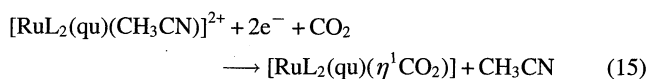
Thus,  $[\text{RuL}(\text{terpy})(\text{CHO})]^+$  is the branch intermediate for two- and multi-electron reduction of  $\text{CO}_2$ . The existence of the feedback path from thermally labile  $[\text{RuL}(\text{terpy})(\text{CHO})]^+$  to stable  $[\text{RuL}(\text{terpy})(\text{CO})]^{2+}$  (as the precursor for  $\text{CO}$  evo-

Scheme 7. Multi-electron reduction of CO<sub>2</sub> catalyzed by [Ru(bpy)<sub>2</sub>(trpy)(CO)]<sup>+</sup>.

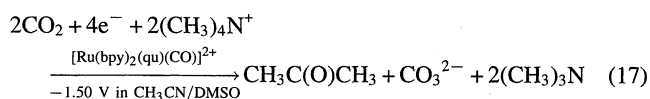
lution) with generating HCOO<sup>-</sup> under CO<sub>2</sub> (Eq. 14) reasonably explains why only CO and/or HCOOH are produced in electro- and photochemical reduction of CO<sub>2</sub> catalyzed by metal complexes reported so far.<sup>5)</sup>

#### Multi-Electron Reduction of CO<sub>2</sub> under Aprotic Conditions

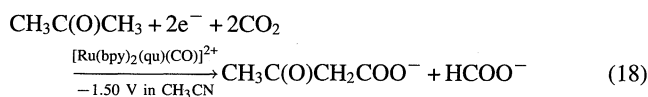
Although [W(CO)<sub>5</sub>(η<sup>1</sup>-CO<sub>2</sub>)]<sup>2-</sup> and [CpFe(CO)<sub>2</sub>(η<sup>1</sup>-CO<sub>2</sub>)]<sup>-</sup> smoothly react with CO<sub>2</sub> to produce [W(CO)<sub>6</sub>] and [CpFe(CO)<sub>3</sub>]<sup>+</sup>,<sup>20a,20b)</sup> these reactions are not suitable for reductive disproportionation reduction of CO<sub>2</sub> because the reduction of W(CO)<sub>6</sub> to [W(CO)<sub>5</sub>]<sup>2-</sup> takes place at potentials more negative than that of the direct reduction of CO<sub>2</sub>. The basicity of [RuL<sub>2</sub>(CO)(η<sup>1</sup>-CO<sub>2</sub>)] is not enough to undergo the oxide transfer reaction by CO<sub>2</sub> so that the equilibrium between [RuL<sub>2</sub>(CO)<sub>2</sub>]<sup>2+</sup> and [RuL<sub>2</sub>(CO)(η<sup>1</sup>-CO<sub>2</sub>)] lies so far to the latter under the normal conditions (Scheme 1). Replacement of a CO ligand of [RuL<sub>2</sub>(CO)(η<sup>1</sup>-CO<sub>2</sub>)] by qu (qu=quinoline) greatly enhances the basicity of the η<sup>1</sup>-CO<sub>2</sub> ligand, since electrochemically prepared [RuL<sub>2</sub>(qu)-(CH<sub>3</sub>CN)]<sup>0</sup> rapidly reacts with CO<sub>2</sub> to give [RuL<sub>2</sub>(qu)-(CO)]<sup>2+</sup> and CO<sub>3</sub><sup>2-</sup> through [RuL<sub>2</sub>(qu)(η<sup>1</sup>-CO<sub>2</sub>)] (Eqs. 15 and 16).<sup>35)</sup>



Indeed, the controlled potential electrolysis of [RuL<sub>2</sub>(qu)-(CH<sub>3</sub>CN)]<sup>2+</sup> (or [RuL<sub>2</sub>(qu)(CO)]<sup>2+</sup>) in the presence of LiBF<sub>4</sub> in CH<sub>3</sub>CN under CO<sub>2</sub> at -1.40 V effectively catalyzes the reductive disproportionation of CO<sub>2</sub> to produce CO and CO<sub>3</sub><sup>2-</sup> under the same electrolysis conditions (Eq. 7). On the other hand, the similar electrochemical reduction of CO<sub>2</sub> using [(CH<sub>3</sub>)<sub>4</sub>N]BF<sub>4</sub> in place of LiBF<sub>4</sub> in CH<sub>3</sub>CN/DMSO at -1.50 V (vs. SCE) produced not only CO<sub>3</sub><sup>2-</sup> and CO (η=42%) but also CH<sub>3</sub>C(O)CH<sub>3</sub>, HCOO<sup>-</sup> and CH<sub>3</sub>C(O)CH<sub>2</sub>COO<sup>-</sup> (η=16, 7, and 6%, respectively) (Eq. 17).



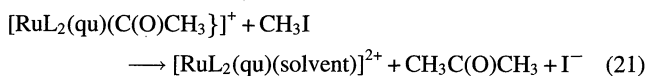
Unexpected formation of CH<sub>3</sub>C(O)CH<sub>3</sub> in the electrochemical CO<sub>2</sub> reduction results from double methylation of [RuL<sub>2</sub>(qu)(CO)]<sup>0</sup> derived from [RuL<sub>2</sub>(qu)(η<sup>1</sup>-CO<sub>2</sub>)]<sup>0</sup>, and both HCOO<sup>-</sup> and CH<sub>3</sub>C(O)CH<sub>2</sub>COO<sup>-</sup> are the products in the electrochemical carboxylation of CH<sub>3</sub>C(O)CH<sub>3</sub> catalyzed by [RuL<sub>2</sub>(qu)(η<sup>1</sup>-CO<sub>2</sub>)] (Eq. 18).



The rate of the formation of CH<sub>3</sub>C(O)CH<sub>3</sub> in the electrochemical reduction of CO<sub>2</sub> (Eq. 17) is remarkably accelerated in the presence of CH<sub>3</sub>I, and only CH<sub>3</sub>C(O)CH<sub>3</sub>, HCOO<sup>-</sup>, and CH<sub>3</sub>C(O)CH<sub>2</sub>COO<sup>-</sup> were produced without evolving CO (Eq. 19).

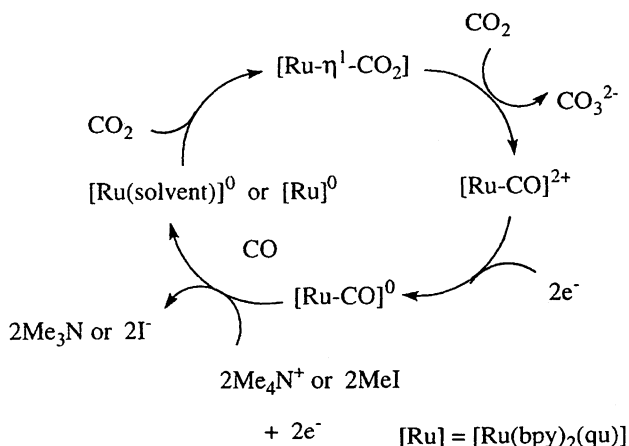


The complete depression of CO evolution in these CO<sub>2</sub> reductions results from smooth formation of [RuL<sub>2</sub>(qu){C(O)CH<sub>3</sub>}]<sup>+</sup> in the reaction of [RuL<sub>2</sub>(qu)(CO)]<sup>0</sup> with CH<sub>3</sub>I prior to the Ru-CO bond breaking (Eqs. 20 and 21).



The mechanism for the formation of CH<sub>3</sub>C(O)CH<sub>3</sub> in the electrochemical reduction of CO<sub>2</sub> catalyzed by [RuL<sub>2</sub>(qu)-(CO)]<sup>2+</sup> is represented in Scheme 8. An electrophilic attack of CO<sub>2</sub> to the two-electron reduced form of [RuL<sub>2</sub>(qu)-(solvent)]<sup>2+</sup> produces [RuL<sub>2</sub>(qu)(η<sup>1</sup>-CO<sub>2</sub>)]<sup>0</sup>. Oxide transfer from [RuL<sub>2</sub>(qu)(η<sup>1</sup>-CO<sub>2</sub>)]<sup>0</sup> to CO<sub>2</sub> generates [RuL<sub>2</sub>(qu)-(CO)]<sup>2+</sup> and CO<sub>3</sub><sup>2-</sup>. Successive alkylation of [RuL<sub>2</sub>(qu)-(CO)]<sup>0</sup> by CH<sub>3</sub>I (or Me<sub>4</sub>N<sup>+</sup>) gives CH<sub>3</sub>C(O)CH<sub>3</sub>. Besides the oxide transfer from [RuL<sub>2</sub>(qu)(CO<sub>2</sub>)]<sup>0</sup> to CO<sub>2</sub>, the complex plays the precursor to HCOO<sup>-</sup> in the presence of CH<sub>3</sub>C(O)CH<sub>3</sub> as a proton source, and the resultant CH<sub>3</sub>C(O)CH<sub>2</sub><sup>-</sup> is trapped by CO<sub>2</sub> to form CH<sub>3</sub>C(O)CH<sub>2</sub>COO<sup>-</sup>. The qu ligand effectively blocks the attack of bulky CH<sub>3</sub>I to Ru, since neither C<sub>2</sub>H<sub>6</sub> nor CH<sub>3</sub>COO<sup>-</sup> was formed in the reduction of CO<sub>2</sub> by [RuL<sub>2</sub>(qu)(CH<sub>3</sub>CN)]<sup>2+</sup>. This was because the





Scheme 8. Catalytic formation of acetone in electrochemical reduction of  $CO_2$  by  $[RuL_2(qu)(solvent)]^{2+}$ .

electrochemical reduction of  $CO_2$  catalyzed by  $[RuL_2(L')-(CH_3CH)]^{2+}$  ( $L'$  = iso-quinoline) in the presence of  $CH_3I$  produced  $C_2H_6$ , which became the main product in the similar  $CO_2$  reduction catalyzed by  $[RuL(terpy)(CO)]^{2+}$  under the similar reaction conditions.

#### Activation of Ru-CO Derived from Ru- $\eta^1$ - $CO_2$

A nucleophilic attack of organic substrates to a CO group of cationic M-CO complexes is widely utilized for carbon-carbon bond formation in organic synthesis. On the other hand, an electrophilic attack of proton and  $CH_3I$  to a CO group of the two-electron reduced form of  $[RuL_2(L')-(CO)]^{2+}$  derived from  $[RuL_2(L')-(CO_2)]^0$  is the key reaction in the multi-electron reduction of  $CO_2$  under electrolysis conditions. The efficiency of the multi-electron reduction of  $CO_2$  accompanied by carbon-carbon bond formation, therefore, is dependent on reductive activation of not only M- $CO_2$  bonds but also M-CO ones. Spectroelectrochemical IR spectra greatly help to understand the reactivity of an M-CO bond depending on the oxidation states of the complexes. The  $\nu(C\equiv O)$  band of  $[RuL_2(qu)(CO)]^{2+}$  at  $2015\text{ cm}^{-1}$  in  $CD_3CN$  undergoes the bathochromic shift to  $1980$  and  $1939\text{ cm}^{-1}$  upon electrochemical one- and two-electron reductions of the complex at  $-1.21$  and  $-1.50\text{ V}$ , respectively (Fig. 4 and Scheme 9). Thus, the ligand (bpy and qu) localized redox reaction of  $[RuL_2(qu)(CO)]^{2+}$  causes the bathochromic shift of  $\nu(CO)$  band by ca.  $40\text{ cm}^{-1}$  per one electron. It is worthy of note that effective depression of CO dissociation from  $[RuL_2(qu)(CO)]^0$ , in contrast to  $[RuL_2(CO)_2]^0$ , is explained by the participation of  $\pi^*$  orbital of qu in the redox reaction. The  $\nu(C\equiv O)$  band at  $1980\text{ cm}^{-1}$  of  $[RuL_2(qu)(CO)]^+$  is not affected by the presence of  $CH_3I$ , while two electron reduction of  $[RuL_2(qu)(CO)]^{2+}$  in the presence of an equiv amount

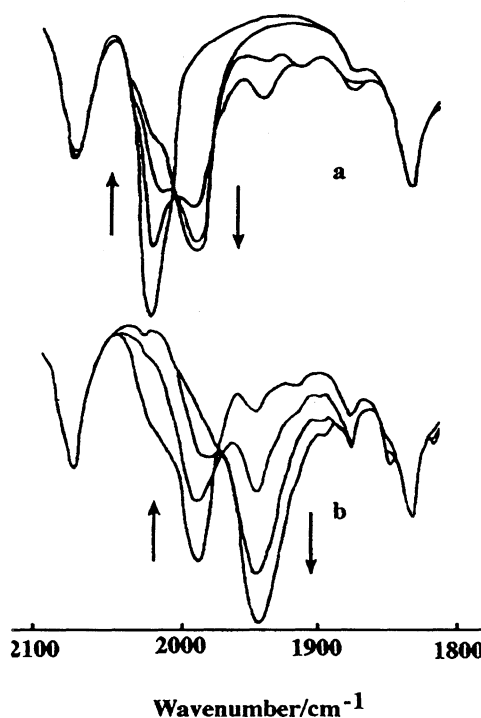
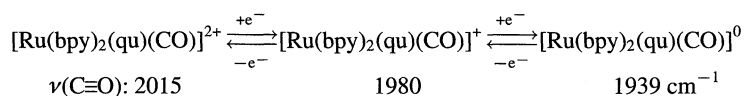


Fig. 4. Time dependent IR spectra of  $[RuL_2(qu)(CO)](PF_6)_2$  under the electrolysis at  $-1.21\text{ V}$  (a) and subsequently at  $-1.50\text{ V}$  in  $CD_3CN$  containing  $LiBF_4$  under  $N_2$ .

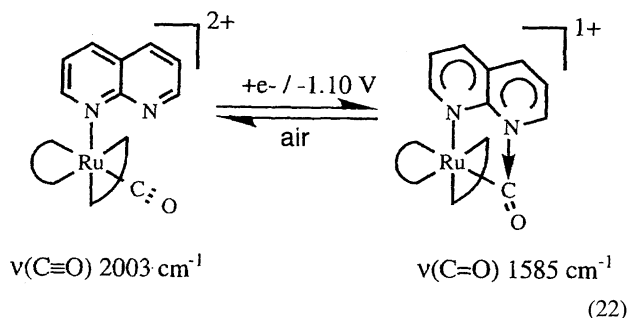
of  $CH_3I$  developed a new  $\nu(C\equiv O)$  band of  $[RuL_2(qu)(C(O)CH_3)]^+$  at  $1568\text{ cm}^{-1}$  as the precursor for  $CH_3C(O)CH_3$  in the electrochemical reduction of  $CO_2$ . It is, however, not clear whether  $[RuL_2(qu)(C(O)CH_3)]^+$  is formed by a direct attack of  $CH_3I$  to the CO group of  $[RuL_2(qu)(CO)]^0$  or by CO insertion to a Ru- $CH_3$  intermediate such as  $[RuL_2(qu)(CH_3)(CO)]^+$ .

Intramolecular cyclization by taking advantage of a ligand localized redox reaction also greatly serves for the reductive activation of M-CO bond derived from M- $CO_2$ . The molecular structure of  $[RuL_2(napy-\kappa N)(CO)]^{2+}$  ( $napy$  = 1,8-naphthyridine) is close to that of  $[RuL_2(qu)(CO)]^{2+}$ . One-electron reduction of the former takes place on the napy ligand at  $-1.03\text{ V}$  (vs.  $Ag/AgCl$ ). Introduction of one-electron into a  $\pi^*$  orbital of the monodentate napy ligand results in a remarkable enhancement of the nucleophilicity of the non-coordinated nitrogen atom. As a result, the  $\nu(C\equiv O)$  band at  $2003\text{ cm}^{-1}$  of  $[RuL_2(napy-\kappa N)(CO)]^{2+}$  shifted to  $1585\text{ cm}^{-1}$  upon one-electron reduction at  $-1.10\text{ V}$  in  $CD_3CN$ . Similar one-electron reduction of  $[RuL_2(napy-\kappa N)(^{13}CO)]-(PF_6)_2$  also caused the red shift of the  $\nu(^{13}C\equiv O)$  band from  $1958$  to  $1543\text{ cm}^{-1}$ . The large red shift of the  $\nu(CO)$  band by  $418\text{ cm}^{-1}$  upon one-electron reduction is associated with the formation of the five-membered carbamoyl ring by an in-



Scheme 9.  $\nu(CO)$  band depending on  $[Ru(bpy)_2(qu)(CO)]^{n+}$  ( $n=0, 1, 2$ ).

tramolecular nucleophilic attack of the non-bonded nitrogen of napy- $\pi$ N to the carbonyl carbon (Eq. 22).<sup>36)</sup>

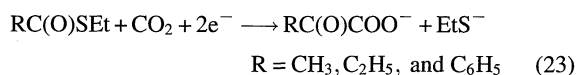


The rate of the  $\text{CH}_3\text{C}(\text{O})\text{CH}_3$  formation in the electrochemical reduction of  $\text{CO}_2$  by using  $(\text{CH}_3)_4\text{N}^+$  as a methylation agent is remarkably increased by participation of the five-membered carbamoyl ring (Eq. 22).

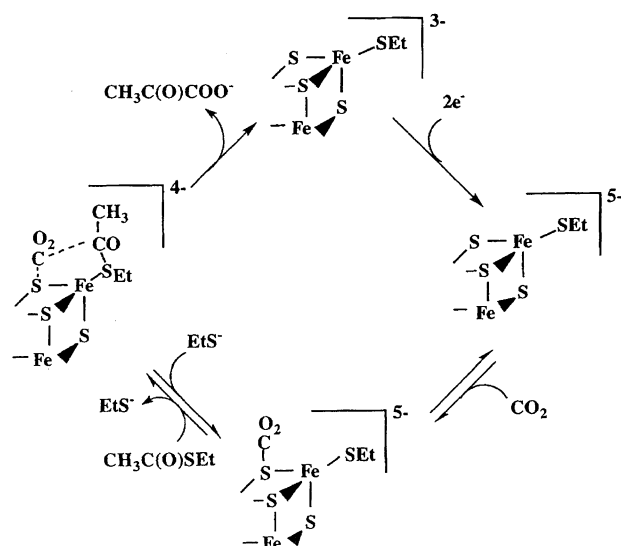
### Activation of $\text{CO}_2$ on Non-Transition Metals

Monomeric  $\text{M}-\eta^1\text{-CO}_2$  complexes may not be suitable species for  $\text{CO}_2$  fixation to organic molecules if one considers a smooth C–O bond cleavage in protic and aprotic media. Such a C–O bond fission is practically inhibited in  $\text{CO}_2$  bonded on organic bases. An electrophilic attack of  $\text{CO}_2$  to O, S, and N atoms of  $\text{M}-\text{XR}$  ( $\text{X}=\text{O}, \text{S}$ ) and  $\text{M}-\text{NR}_2$  groups is usually followed by  $\text{CO}_2$  insertion into these polarized bonds. Accordingly,  $\mu_3\text{-S}$  ligands in an  $\text{M}_3(\mu_3\text{-S})$  moiety may provide feasible binding sites for the activation of  $\text{CO}_2$  without any accompanying C–O bond cleavage, because  $\text{CO}_2$  insertion into an  $\text{M}-\text{S}$  bond of  $\text{M}_3(\mu_3\text{-S})$  cores can probably be neglected due to the steric hindrance.

The  $\text{p}K_a$  values of  $\mu_3\text{-S}$  of  $[\text{Fe}_4(\mu_3\text{-S})_4(\text{SC}_6\text{H}_4\text{C}_n\text{H}_{2n+1})_4]^{3-}$  and  $[\text{Mo}_2\text{Fe}_6(\mu_3\text{-S})_8(\text{SEt})_3(\text{SC}_6\text{H}_4\text{C}_{2n+1})_6]^{5-}$  ( $n=4-12$ ) were determined as ca. 9 and ca. 11, respectively, on the basis of the pH dependent redox reactions of  $[\text{Fe}_4\text{X}_4(\text{YC}_6\text{H}_4\text{C}_n\text{H}_{2n+1})_4]^{2-}$  ( $\text{X}, \text{Y}=\text{S}$  and  $\text{Se}$ ) in aqueous micellar solutions.<sup>37)</sup> In accordance with the difference in the  $\text{p}K_a$  values, strong interaction between  $[\text{Mo}_2\text{Fe}_6\text{S}_8(\text{SEt})_9]^{5-}$  and  $\text{CO}_2$  was confirmed in the cyclic voltammogram (CV) in dry  $\text{CH}_3\text{CN}$ , while no interaction was detected between  $[\text{Fe}_4\text{S}_4(\text{SEt})_4]^{3-}$  and  $\text{CO}_2$  in the same solvent. Furthermore,  $[\text{Mo}_2\text{Fe}_6\text{S}_8(\text{SEt})_9]^{3-}$  catalyzes  $\text{CO}_2$  fixation to  $\text{RC}(\text{O})\text{SEt}$  ( $\text{R}=\text{CH}_3, \text{C}_2\text{H}_5$ , and  $\text{C}_6\text{H}_5$ ) producing  $\text{RC}(\text{O})\text{COO}^-$  without evolving  $\text{CO}$  under the electrolysis at  $-1.50$  V vs. SCE in  $\text{CH}_3\text{CN}$  (Eq. 23).<sup>38)</sup>



Catalytic formation of  $\alpha$ -keto acids by  $\text{CO}_2$  fixation to the carbonyl carbon of  $\text{RC}(\text{O})\text{SR}'$  is essentially the same reaction as the  $\text{CO}_2$  fixation by pyruvate synthase. Based on the reactivity depending on substituents of terminal  $\text{RS}^-$  ligands, the  $\text{CO}_2$  fixation of Eq. 23 is explained in Scheme 10: i) an electrophilic attack of  $\text{CO}_2$  on  $\mu_3\text{-S}$  of  $[\text{Mo}_2\text{Fe}_6(\mu_3\text{-S})_8(\text{SEt})_9]^{5-}$ , ii) substitution of  $\text{EtS}^-$  ligated on Fe by  $\text{RC}(\text{O})\text{SEt}$ , iii) an addition of the reductively activated  $\text{CO}_2$  on sulfur to the carbonyl carbon of  $\text{RC}(\text{O})\text{SEt}$  ligated on Fe. The

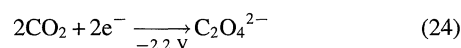


Scheme 10. Proposed path for catalytic formation of  $\alpha$ -keto acids.

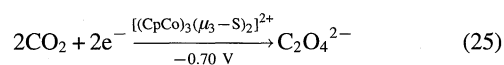
process steps i and ii are supported by the observation that an addition of free  $\text{EtS}^-$  to the solution does not block the  $\text{CO}_2$  adduct formation with  $[\text{Mo}_2\text{Fe}_6\text{S}_8(\text{SEt})_9]^{5-}$ , but strongly interferes with the  $\alpha$ -keto acid formation due to depression of dissociation of  $\text{EtS}^-$  from  $\text{Fe}-\text{SEt}$  group.

### Coupling Reaction of Two $\text{CO}_2$ Molecules Activated on Metal Sulfur Clusters

Oxalate formation attracts much attention from the viewpoints of carbon-carbon bond formation by one- or two-electron reduction of  $\text{CO}_2$ . Uncatalyzed electrochemical reduction of  $\text{CO}_2$  on electrodes produces oxalate through a coupling reaction of  $\text{CO}_2^-$  (Eq. 24).



Savéant et al. have reported that anion radicals of aryl-esters and -nitrils effectively accelerate the coupling reaction of  $\text{CO}_2^-$ , though the redox potentials of those aryl compounds are quite negative and close to that of  $E^\circ(\text{CO}_2/\text{CO}_2^-)$  at  $-2.21$  V (vs. SCE).<sup>39)</sup> A new route for oxalate generation without passing through free  $\text{CO}_2^-$  is, therefore, desired thermodynamically. Two-electron reduction of trinuclear metal-sulfur clusters.  $[(\text{MCp})_3(\mu_3\text{-S})_2]^{2+}$  ( $\text{M}=\text{Co}, \text{Rh}, \text{Ir}$ ) causes an  $\text{M}-\text{M}$  bond cleavage in the  $\text{M}_3(\mu_3\text{-S})$  core. In addition, the basicity of the  $\mu_3\text{-S}$  ligand of  $[(\text{MCp})_3(\mu_3\text{-S})_2]^{2+}$  must be increased upon two-electron reduction. Two-electron reduction of  $[(\text{CpM})_3(\mu_3\text{-S})_2]^{2+}$  may, therefore, create four possible binding sites for an electrophilic attack of  $\text{CO}_2$ . The electrolysis of  $[(\text{CoCp})_3(\mu_3\text{-S})_2]^{2+}$  in  $\text{CO}_2$ -saturated dry  $\text{CH}_3\text{CN}$  at  $-0.70$  V selectively produced  $\text{C}_2\text{O}_4^{2-}$  as a white precipitate (Eq. 25).<sup>41)</sup>



The oxalate formation by the reduction of  $\text{CO}_2$  under the electrolysis at  $-0.7$  V is particularly noteworthy since the

standard redox potential of  $\text{H}_2\text{C}_2\text{O}_4$  is  $-0.475$  V (vs. NHE) in  $\text{H}_2\text{O}$  even at pH 0 ( $25^\circ\text{C}$ ). Similarly, oxalate was selectively produced in the electrochemical reduction of  $\text{CO}_2$  catalyzed by  $[(\text{RhCp}^*)_3(\mu_3\text{-S})_2]^{2+}$  at  $-1.50$  V (vs. SCE) in  $\text{CH}_3\text{CN}$  under  $\text{CO}_2$  atmosphere.<sup>42)</sup> In accordance with this, the two electron reduced forms of  $[(\text{CoCp})_3(\mu_3\text{-S})_2]^{2+}$  and  $[(\text{RhCp}^*)_3(\mu_3\text{-S})_2]^{2+}$  reacted with  $\text{CO}_2$  to produce oxalate in 80 and 60% yields, respectively, with regenerating the oxidized clusters in  $\text{CH}_3\text{CN}$ . In contrast to the reaction of  $[(\text{RhCp}^*)_3(\mu_3\text{-S})_2]^0$  with  $\text{CO}_2$  in  $\text{CH}_3\text{CN}$ ,  $[(\text{IrCp}^*)_3(\mu_3\text{-S})_2]^0$  reacted with the solvent molecule under  $\text{CO}_2$  to give  $[(\text{IrCp}^*)_2(\text{Ir}(\eta^4\text{-Cp}^*\text{CH}_2\text{CN})(\mu_3\text{-S})_2)]^+$  with a linear  $\text{CH}_2\text{CN}$  moiety bonded to a  $\text{Cp}^*$  ring (Fig. 5) and oxalate. The catalytic activity of  $[(\text{IrCp}^*)_2(\text{Ir}(\eta^4\text{-Cp}^*\text{CH}_2\text{CN})(\mu_3\text{-S})_2)]^+$  toward oxalate generation in electrochemical reduction of  $\text{CO}_2$  is much higher than  $[(\text{CoCp})_3(\mu_3\text{-S})_2]^{2+}$  and  $[(\text{RhCp}^*)_3(\mu_3\text{-S})_2]^{2+}$ .

The IR spectra of  $[(\text{RhCp}^*)_3(\mu_3\text{-S})_2]^{2+}$  did not show any interaction with  $\text{CO}_2$  in  $\text{CD}_3\text{CN}$ , while the electrolysis of  $[(\text{RhCp}^*)_3(\mu_3\text{-S})_2]^{2+}$  in  $\text{CO}_2$ -saturated  $\text{CD}_3\text{CN}$  at  $-1.50$  V resulted in appearance of new bands at  $1682$  and  $1605$   $\text{cm}^{-1}$  together with the  $1633$   $\text{cm}^{-1}$  band of oxalate in the solution IR spectra. The  $1680$  and  $1605$   $\text{cm}^{-1}$  bands completely disappeared upon the reoxidation of the solution at  $0.3$  V, and the  $1633$   $\text{cm}^{-1}$  band of oxalate remained unchanged after the reoxidation. The  $1682$  and  $1605$   $\text{cm}^{-1}$  bands shifted to  $1636$  and  $1561$   $\text{cm}^{-1}$ , respectively, when the same electrolysis was conducted under  $^{13}\text{CO}_2$ . On the other hand, the IR spectra of  $[(\text{IrCp}^*)_2(\text{Ir}(\eta^4\text{-Cp}^*\text{CH}_2\text{CN})(\mu_3\text{-S})_2)]^+$  showed a strong peak at  $1680$   $\text{cm}^{-1}$  in  $\text{CO}_2$ -saturated  $\text{CD}_3\text{CN}$ . Moreover, another band emerged around  $1600$   $\text{cm}^{-1}$  upon one-electron reduction of the cluster under the electrolysis at  $-1.50$  V in  $\text{CD}_3\text{CN}$  under  $^{12}\text{CO}_2$ . Prolonged electrolysis of the same solution also resulted in the appearance of the  $1633$   $\text{cm}^{-1}$  band assignable to oxalate. This peak intensified with time. Thus,

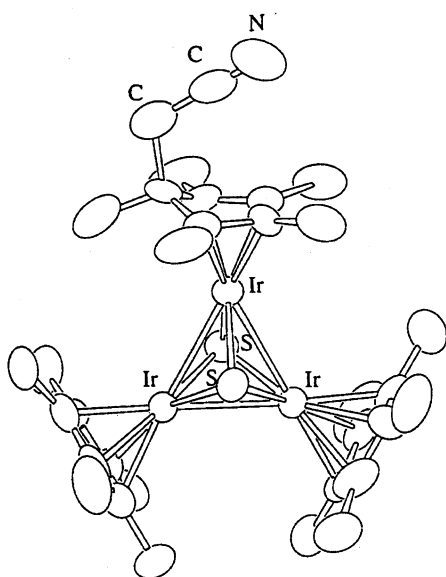


Fig. 5. Crystal structure of  $[(\text{IrCp}^*)_2(\text{IrCp}^*\text{CH}_2\text{CN})(\mu_3\text{-S})_2]^+$  determined by X-ray analysis.

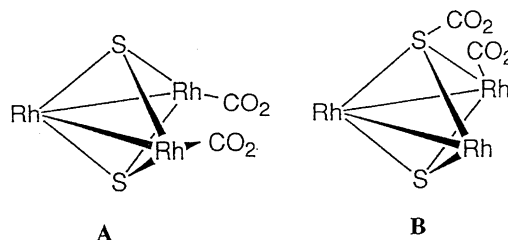


Fig. 6. Two possible structures of 1:2 adducts between  $[(\text{Cp}^*\text{Rh})_3(\mu_3\text{-S})_2]^0$  and  $\text{CO}_2$  as the precursor to  $\text{C}_2\text{O}_4^{2-}$  generation.

the two  $\nu(\text{CO}_2)$  bands at  $1682$  and  $1605$   $\text{cm}^{-1}$  appeared at the same time in the IR spectra of  $[(\text{RhCp}^*)_3(\mu_3\text{-S})_2]^0$  in  $\text{CD}_3\text{CN}$  under  $\text{CO}_2$ , while the former was observed in  $[(\text{IrCp}^*)_2(\text{Ir}(\eta^4\text{-Cp}^*\text{CH}_2\text{CN})(\mu_3\text{-S})_2)]^+$  and the latter emerged in the IR spectra of  $[(\text{IrCp}^*)_2(\text{Ir}(\eta^4\text{-Cp}^*\text{CH}_2\text{CN})(\mu_3\text{-S})_2)]^0$  in  $\text{CD}_3\text{CN}$  under  $\text{CO}_2$ . These results indicate that  $[(\text{RhCp}^*)_3(\mu_3\text{-S})_2]^0$  forms a 1:2 adduct with  $\text{CO}_2$  as a precursor to oxalate.

If  $\text{CO}_2$  is linked to  $[(\text{RhCp}^*)_3(\mu_3\text{-S})_2]^0$  with an  $\eta^1$ -mode, the OCO angle ( $2\alpha$ ) of an adduct is expressed by Eq. 26,<sup>43)</sup>

$$\left(\frac{\nu^i}{\nu}\right)^2 = \left(\frac{M_C}{M_C^i}\right) \left(\frac{M_C^i + 2M_O \sin^2 \alpha}{M_C + 2M_O \sin^2 \alpha}\right) \quad (26)$$

in which  $\nu^i$  and  $\nu$  represent the  $\nu_{\text{asym}}(^{13}\text{CO}_2)$  and  $\nu_{\text{asym}}(^{12}\text{CO}_2)$  bands ( $\text{cm}^{-1}$ ), and  $M_C^i$ ,  $M_C$ , and  $M_O$  are the mass number of  $^{13}\text{C}$ ,  $^{12}\text{C}$ , and  $^{16}\text{O}$ , respectively. On the basis of the  $\nu_{\text{asym}}(^{12}\text{CO}_2)$  at  $1682$  and  $1605$   $\text{cm}^{-1}$ , the OCO angles of those  $\text{CO}_2$  molecules linked to  $[(\text{RhCp}^*)_3(\mu_3\text{-S})_2]^0$  are estimated as  $157$  and  $132^\circ$ , respectively. The latter is quite close to the OCO angle of  $[\text{Co}(\text{Pr-salen})(\text{CO}_2\text{Na})]^+$  ( $135^\circ$ ).

There are two possibilities for the binding sites for the attack of two  $\text{CO}_2$  molecules to  $[(\text{RhCp}^*)_3(\mu_3\text{-S})_2]^0$  (Fig. 6); one is two coordinatively unsaturated Rh atoms produced by a Rh–Rh bond fission by the two-electron reduction of the cluster and the other is Rh and  $\mu_3\text{-S}$ . Ligation of two  $\text{CO}_2$  to two Rh must be sterically blocked by bulky two  $\text{Cp}^*$  ligands (Fig. 6A). On the other hand, there seems to be no serious steric hindrance for the attack of  $\text{CO}_2$  to  $\mu_3\text{-S}$ . The appearance of a strong band at  $1680$   $\text{cm}^{-1}$  in the IR spectra of  $[(\text{IrCp}^*)_2(\text{IrCp}^*\text{CH}_2\text{CN})(\mu_3\text{-S})_2]^+$  in  $\text{CO}_2$ -saturated  $\text{CD}_3\text{CN}$  also supports an electrophilic attack of  $\text{CO}_2$  to  $\mu_3\text{-S}$  of  $[(\text{RhCp}^*)_3(\mu_3\text{-S})_2]^0$ . Non-equivalence of two  $\text{CO}_2$  molecules in the IR spectra, therefore, is explained by the attack of  $\text{CO}_2$  molecules to Rh and S (Fig. 4B). The oxalate formation in the electrochemical reduction of  $\text{CO}_2$  catalyzed by  $[(\text{MCp})_3(\mu_3\text{-S})_2]^0$ , therefore, is attributed to the coupling reaction of two  $\text{CO}_2$  molecules bonded on the adjacent M and S atoms.

## References

- 1) a) "Molecular Electrochemistry of Inorganic, Bioorganic and Organometallic Compounds," ed by C. Amatore, A. Jutand, and M. F. Nielsen, NATO ASI Ser. C (1993), 307; b) "Chemical Fixation of Carbon Dioxide," ed by M. M. Halmann, CRC Press, London (1993).
- 2) a) "Enzymatic and Model Carboxylation and Reduction Re-

- actions for Carbon Dioxide," ed by M. Arest and J. V. Schloss, NATO Ser. C (1993); b) S. Derien, J. C. Clinet, E. Dunach, and J. Perichon, *J. Org. Chem.*, **58**, 2578 (1993); c) D. Sylvie, E. Dunach, and J. Perichon, *J. Am. Chem. Soc.*, **113**, 8447 (1991).
- 3) M. Aresta, C. F. Nobile, V. G. Albano, E. Fomi, and M. Manassero, *J. Chem. Soc., Chem. Commun.*, **1975**, 636.
- 4) a) D. H. Gibson, *Chem. Rev.*, **96**, 2063 (1996); b) J. Constamagna, G. Ferraudi, J. Canales, and J. Vergas, *Coord. Chem. Rev.*, **148**, 221 (1996).
- 5) a) H. Nakajima, T. Mizukawa, H. Nagao, and K. Tanaka, *Chem. Lett.*, **1995**, 251; b) K.-M. Lam, K.-Y. Wong, S.-M. Yang, and C.-M. Che, *J. Chem. Soc., Dalton Trans.*, **1995**, 1103; c) J. Costamagna, J. Canales, J. Vargas, and G. Ferraudi, *Pure Appl. Chem.*, **67**, 1045 (1995); d) A. M. Herring, B. D. Steffey, A. Miedaner, S. A. Wander, and D. L. DuBois, *Inorg. Chem.*, **34**, 1100 (1995); f) B. D. Steffey, A. Miedaner, M. L. Maciejewski-Farmer, P. R. Bernatis, A. M. Herring, V. S. Allured, V. Carperos, and D. L. DuBois, *Organometallics*, **13**, 4844 (1994); g) A. Szymaszek and F. Pruchnik, *Rhodium Express*, **5**, 18 (1994); h) E. Fujita, J. Haff, R. Sanzenbacher, and H. Elias, *Inorg. Chem.*, **33**, 4627 (1994); i) K. Ogura, H. Sugihara, J. Yano, and M. Higasa, *J. Electrochem. Soc.*, **141**, 419 (1994); j) E. Kimura, S. Wada, M. Shionoya, and Y. Okazaki, *Inorg. Chem.*, **33**, 770 (1994); k) R. J. Haines, R. E. Wittrig, and C. P. Kubiak, *Inorg. Chem.*, **33**, 4723 (1994); l) T. Ogata, Y. Yamamoto, Y. Wada, K. Murakoshi, M. Kusaba, N. Nakashima, A. Ishida, S. Takamuku, and S. Yanagida, *J. Phys. Chem.*, **99**, 11916 (1995); m) O. Ishitani, M. W. George, T. Ibusuki, F. P. A. Johnson, K. Koike, K. Nozaki, C. Pac, J. J. Turner, and J. R. Westwell, *Inorg. Chem.*, **33**, 4712 (1994), and references therein.
- 6) Y. Musashi, T. Hamada, and S. Sakaki, *J. Am. Chem. Soc.*, **117**, 11320 (1995).
- 7) a) S. Gambarotta, F. Arena, C. Floriani, and P. F. Zanazzi, *J. Am. Chem. Soc.*, **104**, 5914 (1982); b) J. C. Calabrese, T. Herskovitz, and J. B. Kinney, *J. Am. Chem. Soc.*, **105**, 5914 (1983).
- 8) a) D. A. Gangi and R. R. Durand, Jr., *J. Chem. Soc., Chem. Commun.*, **1986**, 697; b) D. J. Pearce and D. Pletcher, *J. Electroanal. Chem.*, **197**, 317 (1986); c) M. H. Schmidt, G. M. Miskelly, and N. S. Lewis, *J. Am. Chem. Soc.*, **112**, 3420 (1990); d) C. Creutz, H. A. Schwarz, J. F. Wishart, E. Fujita, and N. Sutin, *J. Am. Chem. Soc.*, **111**, 1153 (1989); e) N. Katz, D. J. Szalda, M. H. Chou, C. Creutz, and N. Sutin, *J. Am. Chem. Soc.*, **110**, 6591 (1988).
- 9) C. Creutz, in "Electrochemical and Electrocatalytic Reactions of Carbon Dioxide," ed by B. P. Sullivan, K. Krist, and H. E. Guard, Elsevier, Amsterdam (1993), p. 55.
- 10) J. M. Maher and N. J. Cooper, *J. Am. Chem. Soc.*, **102**, 7606 (1980).
- 11) G. R. Lee and N. J. Cooper, *Organometallics*, **4**, 794 (1985).
- 12) T. Herskovitz, *J. Am. Chem. Soc.*, **99**, 2391 (1977).
- 13) K. Tanaka, M. Morimoto, and T. Tanaka, *Chem. Lett.*, **1983**, 901.
- 14) D. H. Gibson and T.-S. Ong, *J. Am. Chem. Soc.*, **109**, 7191 (1987).
- 15) a) J. R. Sweet and W. A. G. Graham, *Organometallics*, **1**, 982 (1982); b) C. P. Casey, M. A. Andrews, and J. E. Rinz, *J. Am. Chem. Soc.*, **101**, 741 (1979).
- 16) K. Bowman, A. J. Deeming, and G. P. Proud, *J. Chem. Soc., Dalton Trans.*, **1985**, 857.
- 17) H. Tanaka, B.-C. Tzeng, H. Nagao, S.-M. Peng, and K. Tanaka, *Inorg. Chem.*, **32**, 1508 (1993).
- 18) K. Toyohara, H. Nagao, T. Adachi, T. Yoshida, and K. Tanaka, *Chem. Lett.*, **1996**, 27.
- 19) C. Amatore and J.-M. Saveant, *J. Am. Chem. Soc.*, **103**, 5021 (1981).
- 20) J. R. Pinkes, C. J. Masi, R. Chiulli, B. D. Steffey, and A. R. Cutler, *Inorg. Chem.*, **36**, 70 (1997).
- 21) H. Nakajima, K. Tsuge, and K. Tanaka, *Chem. Lett.*, **1997**, 485.
- 22) D. M. Kern, *J. Chem. Educ.*, **37**, 14 (1960).
- 23) J. Hawecker, J.-M. Lehn, and R. Ziessel, *J. Chem. Soc., Chem. Commun.*, **1984**, 328.
- 24) a) i) B. P. Sullivan, C. M. Bolinger, D. Conrad, W. J. Vining, and T. J. Meyer, *J. Chem. Soc., Chem. Commun.*, **1985**, 1414; b) T. R. O'Toole, B. P. Sullivan, M. R. -M. Bruce, L. Margerum, R. W. Murray, and T. J. Meyer, *J. Electroanal. Chem.*, **217**, 259 (1989); c) P. Christensen, A. Hamnett, A. V. G. Muir, and J. A. Timney, *J. Chem. Soc., Dalton Trans.*, **1992**, 1455.
- 25) F. P. A. Johnson, M. W. George, F. Hartl, and J. J. Turner, *Organometallics*, **15**, 3374 (1996).
- 26) a) H. Ishida, K. Tanaka, and T. Yanaka, *Organometallics*, **6**, 181 (1987); b) H. Ishida, H. Tanaka, K. Tanaka, and T. Tanaka, *J. Chem. Soc., Chem. Commun.*, **1987**, 131.
- 27) H. Ishida, K. Tanaka, and T. Tanaka, *Inorg. Chem.*, **6**, 553 (1987).
- 28) J. R. Pugh, M. R. M. Bruce, B. P. Sullivan, and T. J. Meyer, *Inorg. Chem.*, **30**, 86 (1991).
- 29) M. Beley, J.-P. Collin, R. Ruppert, and J.-P. Sauvage, *J. Am. Chem. Soc.*, **106**, 7461 (1986).
- 30) a) S. Sakaki, *J. Am. Chem. Soc.*, **112**, 7813 (1990); b) **114**, 2055 (1992).
- 31) E. Fujita, J. Haff, R. Sanzenbacher, and H. Elias, *Inorg. Chem.*, **33**, 4627 (1994).
- 32) S. Chardon-Noblat, M.-N. Collomb-Dunand-Sauthier, A. Deronzier, R. Ziessel, and D. Zsoldos, *Inorg. Chem.*, **33**, 4410 (1994).
- 33) a) P. M. Treichel and R. L. Schubhin, *Inorg. Chem.*, **6**, 1328 (1967); b) C. Lapinte and D. Astruc, *J. Chem. Soc., Chem. Commun.*, **1983**, 430; c) C. Lapinte, D. Catheline, and D. Astruc, *Organometallics*, **7**, 1683 (1988).
- 34) H. Nagao, T. Mizukawa, and K. Tanaka, *Inorg. Chem.*, **33**, 3415 (1994).
- 35) H. Nakajima, Y. Kushi, H. Nagao, and K. Tanaka, *Organometallics*, **14**, 5093 (1995).
- 36) H. Nakajima and K. Tanaka, *Chem. Lett.*, **1995**, 891.
- 37) a) K. Tanaka, T. Tanaka, and I. Kawafune, *Inorg. Chem.*, **23**, 516 (1984); b) K. Tanaka, and M. Moriya, and T. Tanaka, *Inorg. Chem.*, **25**, 835 (1986); c) M. Nakamoto, K. Tanaka, and T. Tanaka, *Bull. Chem. Soc. Jpn.*, **61**, 4099 (1989).
- 38) N. Komeda, H. Nagao, T. Matsui, G. Adachi, and K. Tanaka, *J. Am. Chem. Soc.*, **114**, 3625 (1992).
- 39) A. Gennaro, A. A. Isse, J.-M. Savéant, M.-G. Severin, and E. Vianello, *J. Am. Chem. Soc.*, **118**, 7190 (1996).
- 40) a) C. R. Pulliam, J. B. Thoden, A. M. Stacy, B. Spencer, M. H. Englert, and L. F. Dahl, *J. Am. Chem. Soc.*, **113**, 7398 (1991); b) A. Venturrelli and T. B. Rauchfuss, *J. Am. Chem. Soc.*, **116**, 4824 (1994).
- 41) a) Y. Kushi, H. Nagao, T. Nishioka, K. Isobe, and K. Tanaka, *J. Chem. Soc., Chem. Commun.*, **1995**, 1223.
- 42) Y. Kushi, H. Nagao, T. Nishioka, K. Isobe, and K. Tanaka, *Chem. Lett.*, **1994**, 2175.
- 43) K. Nakamoto, "Infrared and Raman Spectra of Inorganic and Coordination Compounds," Wiley-Interscience Publication, New York (1986).



Koji Tanaka, Ph. D., Professor of Institute for Molecular Science: born in Osaka in 1946. He obtained his B. Sc. in Chemistry from Osaka University in 1969. After he finished his master's course in 1971, he was immediately promoted to an assistant professor in the Department of Chemistry, Faculty of Engineering, Osaka University. He received his Ph. D. for research in metal complexes with chalcogenide ligands with the late Professor Toshio Tanaka in 1975. From 1978 to 1979, he studied Fischer-Tropsch reactions with Prof. R. B. King in Georgia University. Since then, he has worked on redox reactions of bioinorganic compounds. In 1990 he was promoted to an associate professor of Osaka University, and then moved to the Institute for Molecular Science as a full professor in the same year. His current research is focused on transformation of stable small molecules driven by redox reactions of metal complexes.